# 20

JEAN SURDEJ* AND JEAN-FRANÇOIS CLAESKENS*

# Gravitational lensing

In his theory of general relativity (GR), Einstein established that a massive object curves space–time and that photons move along geodesics of this curved space. Einstein's prediction was confirmed during the solar eclipse of 1919. This not only provided a decisive, quantitative proof of the validity of GR but also gave confirmation of the concept that electromagnetic waves do undergo deflections in gravitational fields.

Atmospheric lensing effects may lead to a distortion or to the formation of multiple images of a distant source, resulting in the perception of a 'mirage'. They sometimes literally deform our view of the surrounding areas. Similarly, gravitational lensing may perturb our view of the distant Universe and affect our physical understanding of various classes of extragalactic objects. The great interest in gravitational lensing comes from the fact that this phenomenon can be used as an astrophysical and cosmological tool. Indeed, gravitational lensing may help in deriving:

1. the distance scale of the Universe – via the determination of the Hubble constant $H_0$ – and possibly the values of other cosmological parameters (the cosmological density $\Omega_0$ and the cosmological constant $\lambda_0$),
2. the mass distribution $M(r)$ of the lens,
3. the extinction law in the deflector, usually located at high redshift,
4. the nature and distribution of luminous and dark matter in the Universe,
5. the size and structure of quasars,
6. the size of absorbing intergalactic gas clouds,
7. upper limits on the density of a cosmological population of massive compact objects.

In this chapter we summarize some of the theoretical and observational evidence supporting these claims and show how space observations have significantly contributed in some of the areas listed above.

The chapter is organized as follows. We first review the historical background of gravitational lensing in Section 1. Unlike most other astrophysical discoveries made during the last century, the physics of gravitational lensing was understood well before the first example of a multiply-imaged extragalactic object was found.

In Section 2 we describe the basic principles and concepts of gravitational lensing. We first establish the exact form of the lens equation. By making use of the Einstein deflection angle, we derive the expression for the angular diameter of an Einstein ring, which is also the typical angular separation between multiply-lensed images when the conditions of perfect alignment between the observer, the lens and the source are no longer fulfilled. We then set up a sufficient condition for an observer to see an Einstein ring, or multiple images, of a distant source that is located behind a deflector, and go on to derive, for the case of a point-mass lens model, expressions for the expected image positions and their amplifications. Using wavefront and ray tracing diagrams, we introduce the important concepts of caustics and time delays. We then show how all the lensed image configurations observed in the Universe may be understood in terms of the relative location between the observer and the caustics associated with an asymmetric lens. Several outstanding

* Université de Liège, Liège, Belgium

*Jean Surdej and Jean-François Claeskens, The Century of Space Science, 441–469*

examples of gravitational lens systems observed with the Hubble Space Telescope (HST) serve as illustrations.

In Section 3, we discuss the most remarkable astrophysical and cosmological applications of gravitational lensing. These include the independent determination of the Hubble constant $H_0$ based upon the measurement of the time delay $\Delta t$ between the observed light curves of multiply-imaged quasars. The possibility of weighing the mass of lensing galaxies, galaxy clusters and intervening dark matter from the observation of multiply-imaged distant sources, arcs and arclets is also reviewed. We further discuss the possibility of using gravitational lensing to determine the cosmological density $\Omega_0$ ($=8\pi G\rho_0/3H_0^2$) and the reduced cosmological constant $\lambda_0$ ($=\Lambda c^2/3H_0^2$) of the Universe, the cosmological density $\Omega_L$ of dark compact lenses, the size of intergalactic absorbing clouds, dust extinction laws in deflecting galaxies and the structure and size of quasars. We also present the status of optical searches for massive astrophysical compact halo objects (MACHOs) based upon microlensing, the formation of giant luminous arcs in galaxy clusters and the observation of 'weak lensing' in the Universe.

The anticipated contributions of ongoing and future space missions such as Chandra, XMM-Newton, MAP, FIRST-Herschel, Planck, NGST and GAIA are presented in Section 4.

## 1 HISTORICAL BACKGROUND

One of the consequences of the theory of GR is that light rays are deflected in gravitational fields. Although this prediction was made in the twentieth century, speculations that light rays might be bent by gravitation had been proposed much earlier. Indeed, considering that light is composed of elementary constituents, Isaac Newton suggested as early as 1704 that the gravitational field of a massive object could possibly bend light rays, just as it would alter the trajectory of material particles. A century later, Laplace independently made this same suggestion. Furthermore, the astronomer Johann von Soldner (1804) at the Munich Observatory found that, in the framework of Newtonian mechanics, a light ray passing near the limb of the Sun should undergo an angular deflection of 0.875″. However, because the wave description of light prevailed during the eighteenth and nineteenth centuries, neither the conjecture of Newton nor the result of Soldner were ever taken seriously. In 1911 Albert Einstein had re-derived the latter result on the basis of the equivalence principle, unaware of Soldner's work.

In the elaboration of his theory of GR, Einstein predicted that a massive object curves spacetime in its vicinity and that any free particle, massive or not (e.g. photons), will move along geodesics of this curved space. After deriving the full field equations of GR, he predicted in 1915 that a light ray passing near the solar limb should be deflected by an angle given by

$$\hat{\alpha} = 4GM/(c^2R) \ll 1 \tag{1}$$

where $G$ is the gravitational constant, $c$ is the velocity of light and $M$ and $R$ are the mass and radius of the Sun (or of any other compact lens), respectively. This deflection angle turns out to be exactly twice the value derived by Soldner and by Einstein himself in 1911; the factor of 2 merely reflects the metric curvature. Note that in Newtonian terms the Einstein deflection also follows if one assumes a refractive index $n$ associated with the Newtonian gravitational potential $U$ ($|U| \ll c^2$) via the relation

$$n = 1 - 2U/c^2 \tag{2}$$

The analogy between atmospheric and gravitational lensing then becomes obvious. Note, however, that the bending of light rays in gravitational fields is predicted to be totally 'achromatic' (see eqn (1)).

Using photographs of a stellar field taken during the solar eclipse in May 1919, and six months apart, Arthur Eddington and his collaborators (Dyson *et al.* 1920) were able to confirm, within a 20–30% uncertainty, the deflection angle predicted by Einstein (Figure 1). This was the second correct prediction of GR – the successful interpretation of the advance of Mercury's perihelion being the first – and marked the full acceptance of the work of Einstein.

It seems that Eddington (1920) was the first to propose the possible formation of multiple images of a background star by the gravitational lensing effect of a foreground one (but see the finding by Renn *et al.* (1997)). Note, however, that Oliver Lodge (1919) had already characterized massive

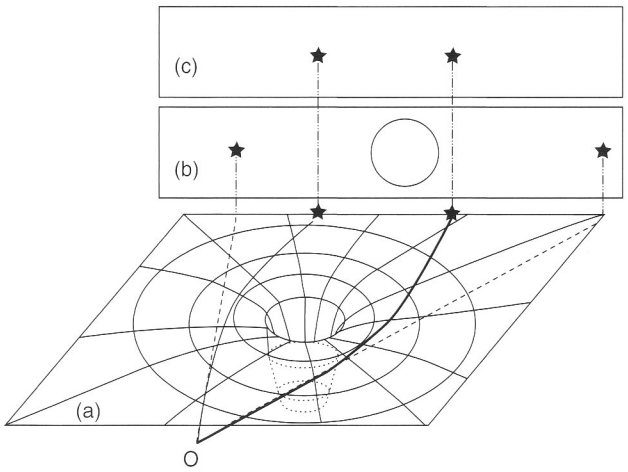


**Figure 1** Curved spacetime around the Sun (a) and deflection of light rays from two distant stars as seen by an observer (O) during a solar eclipse (b) and six months apart (c).

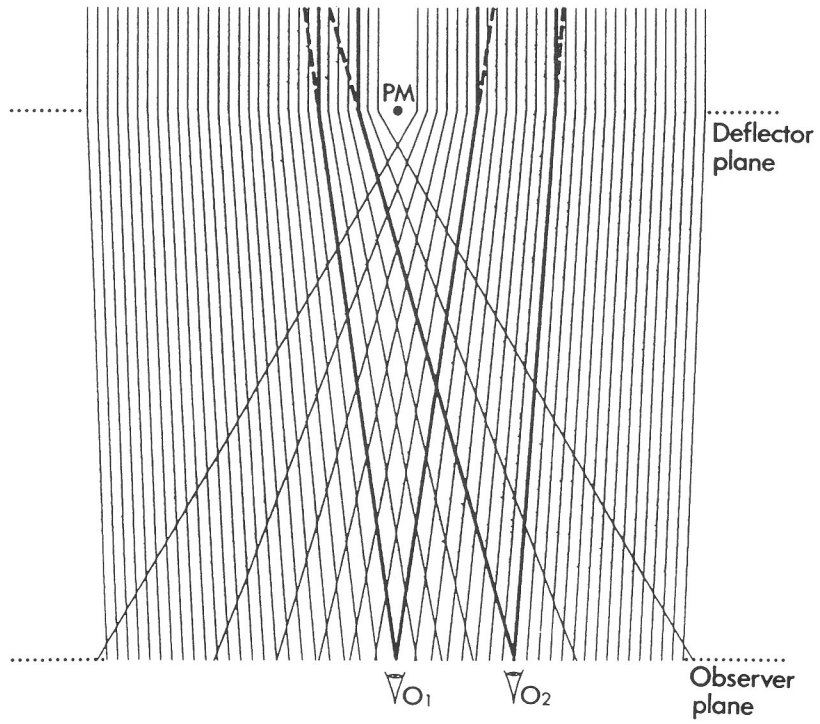


**Figure 2** The paths of light rays in a point-mass (PM) lens model. In accordance with eqn (1), a set of parallel rays emitted from a distant source are deflected from their original paths as they cross the deflector plane. Different observer positions are represented from where an Einstein ring ($O_1$) or a double image ($O_2$) may be seen.

objects like the Sun as imperfect focusing lenses since they had no real focal length; the light from a background object being mainly concentrated along a focal line of 'infinite' length (Figure 2). In 1923, E.B. Frost, then director of the Yerkes Observatory, initiated a programme to search for multiple images of stars in the Galaxy, but it seems that these observations never really took place. Orest Chwolson (1924) suggested that, in the case of a perfect alignment between an observer and two stars located at different distances, the observer should see a ring-shaped image of the background star around the foreground one.

Independently, at the request of Rudi W. Mandl, a Czech electrical engineer, Einstein (1936) rediscovered the major characteristics (double images, the 'Chwolson' ring usually referred to as the 'Einstein' ring, and so on) of one star lensed by another, but he was very sceptical about the possibility of observing this phenomenon among stars, probably because the expected angular separations between the lensed images were so small. What seems remarkable is that Einstein had first established the whole theory of the formation of multiply-lensed images (the lensing equation, formation of double images by a point-like deflector, amplification of the lensed images, and so on) during the spring of 1912, three years before completing his theory of GR. This finding has recently been reported by Renn *et al.* (1997), who had examined some of Einstein's notebooks. It does therefore seem that by 1936 Einstein had totally forgotten his pioneering gravitational lensing work from 1912, as if he had already convinced himself that the idea was too speculative to have any chance of empirical confirmation.

Fritz Zwicky (1937a,b) was the first to realize the very high probability of identifying a gravitational lens mirage, (i.e. one composed of several distinct images of a single object) among extragalactic sources. He even proposed to use galaxies as natural cosmic telescopes to observe otherwise too faint and distant background objects. He also emphasized the possibility of determining the mass of distant galaxies simply by applying gravitational lens optometry and, in addition, to test the theory of GR. In 1937 Zwicky stated that 'the probability that galactic nebulae which act as gravitational lenses will be found becomes practically a certainty', and he was therefore very much surprised some twenty years later that no such lensing effects had yet been found with the 5 m (200-inch) Hale Telescope at Palomar (Zwicky 1957).

After several decades of little activity, interest in the theory of gravitational lenses was revived by Klimov (1963), Liebes (1964) and Refsdal (1964a,b, 1966a). Some of their proposed applications were particularly promising because of the recent discovery of quasars by Maarten Schmidt

(1963). It would indeed be much easier to prove the lensing origin of multiple QSO images rather than that of extended and diffuse galaxy images, since the former ones consist of very distant, luminous and star-like objects. (For more details on quasars, see Peterson (1997).) In 1964 Sjur Refsdal proposed to apply geometric optics in order to estimate the time delay between the arrival times of two parts of the same distorted wavefront at the observer; this proposal, which formed the second part of his master's thesis, was (erroneously) judged of uncertain quality by his supervisor. Nevertheless he succeeded in publishing his findings (Refsdal 1964a,b); the referee of these papers was Dennis Sciama! Refsdal finally, obtained his Ph.D. in 1970 on the basis of that controversial second part of his master's thesis.

On the basis of the strong similarity between the spectra of quasars and of the nuclei of Class 1 Seyfert galaxies, Barnothy (1965) proposed that high-redshift quasars could actually be the lensed images of distant Class 1 Seyfert galactic nuclei. Sanitt (1971) criticized this view on the basis of statistical arguments.

Theoretical work continued at a low level of activity through the 1970s. Refsdal (1965, 1970) and Press and Gunn (1973) discussed problems on lens statistics, Bourassa and Kantowski (1975) considered extended non-symmetric lenses (Bourassa *et al.* 1973) and Dyer and Roeder (1972) derived a distance–redshift relation for the case of inhomogeneous universes. In spite of clear theoretical predictions, the interest from observers was largely absent, and no systematic search for lenses was initiated.

Forty-two years after Zwicky's prediction, the first example of a distant quasar (Q0957 + 561) doubly imaged by a foreground massive lensing galaxy and its attendant galaxy cluster was serendipitously discovered by Walsh *et al.* (1979). This system consists of two lensed quasar images separated by approximately 6″. Good evidence that Q0957 + 561 A and B correspond to twin lensed images of a single quasar was provided by

1. the similarity between their spectra,
2. a simple lens model which could naturally account for the slight morphological differences detected between the optical and radio images of the quasar (Young *et al.* 1981),
3. the discovery of the lensing galaxy between the twin quasar images, made possible by the use of modern CCD imaging,
4. the observation of a time delay of 1.14 years, first reported by Vanderriest *et al.* (1989), between the light variations of the two quasar components.

In parallel with the discovery of several other multiply-imaged quasars, an even stronger interest in gravitational lensing studies developed with the first identification of giant luminous arcs in 1986, by two independent teams (Section 3.5). Since 1982 a group of French astronomers led by L. Nottale from Meudon Observatory had regularly submitted observing proposals with the Canada–France–Hawaii Telescope (CFHT) to search for such arcs in the centres of rich and compact galaxy clusters, among them Abell 370. However, the observing programme committees were not at all receptive to this kind of proposition. Although these predictions were entirely based on the theory of GR, and had been promoted several decades earlier by Zwicky, they probably still looked too revolutionary to conservative observing programme committee members. Furthermore, during the first international conference that was explicitly dedicated to the field of gravitational lensing, entitled 'Quasars and Gravitational Lenses' (24th Liège International Astrophysical Colloquium, 1983), some of the organizers were very surprised by the high degree of scepticism that was still present among a significant number of the participants. Probably half the audience still then considered gravitational lensing to be an unproved phenomenon, while many others thought that the proposed lensed monsters would remain a mere cosmic curiosity, with no further scientific interest. It also seems that until the 1980s, in some institutes gravitational lensing was not always regarded as an acceptable subject to study. Astronomers who wished to pursue the subject would not have received a research grant for work dedicated to gravitational lensing – nor would they be invited to deliver a seminar on the topic. We know from Refsdal, Nottale and many other pioneers that they had the feeling of being considered somewhat heretic by some of their colleagues.

Following the pioneering detections of multiply-imaged quasars and giant luminous arcs, the levels of observational as well as theoretical activities have increased dramatically. More than fifty multiply-imaged quasars and an even larger number of gravitational arcs have now been discovered, and more than 3100 scientific publications have been written over the past twenty years on the subject of gravitational lensing (Figure 3). Space observations, and in particular

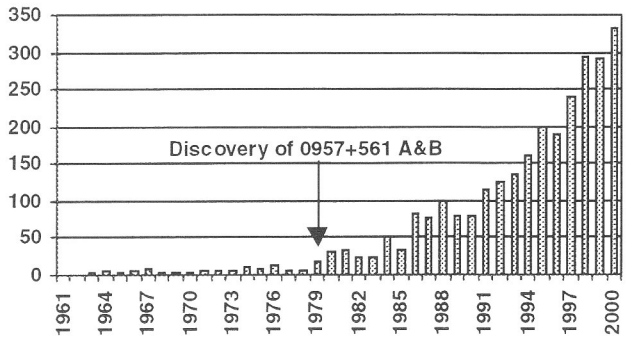


**Figure 3** The number of scientific papers published annually on gravitational lensing over the past forty years. (Based on the gravitational lensing bibliography compiled by Pospieszalska-Surdej *et al.* (2000).)

direct imaging with the HST, have contributed decisively to our present understanding of gravitational lensing effects.

Gravitational lensing constitutes now a very important branch of galactic, extragalactic and cosmological astrophysics. There is no doubt that because of the intimate link between the curvature of spacetime and gravitational lensing at all scales and all locations in the Universe, and because of the new technologies and space missions planned for the twenty-first century, our physical understanding of the cosmos will continue to ever increase.

The reader is referred to Schneider *et al.* (1992) for a more detailed account of the history of gravitational lensing, as well as for a more complete and theoretical presentation of this subject.

## 2 THE PHYSICS OF GRAVITATIONAL LENSING AND SOME IMPORTANT CONCEPTS

The first step in understanding the properties of the images of a lensed source, is to set up the lens equation. We then establish the important relation between the angular diameter of the Einstein ring and the mass of the deflector, and find a sufficient condition for a potential deflector to produce multiple images of a distant source. For a point-mass lens model, we derive expressions for the image positions and amplifications. By means of ray and wavefront tracing diagrams we introduce the concepts of caustics and time delays. Finally, with the help of a gravitational lens simulator, we show how it is possible to reproduce all image configurations that have been observed for the known gravitational lens systems.

### 2.1 The lens equation and multiple imaging

Along the line of sight to a distant source, there is usually only one mass concentration which acts as a lens, and its size is very much smaller than the distances between the source and the lens, and between the lens and the observer (Figure 4). It is thus reasonable to adopt the 'thin lens approximation', according to which the deflection of a light ray takes place near the deflector at the precise location where the ray crosses the plane perpendicular to the observer–deflector direction. This plane is referred to as the 'lens plane', and the parallel plane containing the source is called the 'source plane'. Furthermore, geometric optics can be used since physical optical effects, induced by optical path differences, are negligible in all realistic situations. Under these assumptions, and given the achromatic property of the gravitational deflection of light, all lensing effects previously described may directly be understood from the lens equation (Figure 4).

Let us define the true position of the source S on the sky by the angle vector $\boldsymbol{\theta}_s$ and the image position(s) by $\boldsymbol{\theta}_i$ ($i = 1, 2, \ldots$). These correspond to the solutions of the lens equation

$$\boldsymbol{\theta} - \boldsymbol{\theta}_s = \boldsymbol{\alpha}(\boldsymbol{\theta}) = (D_{ds}/D_{os})\hat{\boldsymbol{\alpha}}(\boldsymbol{\theta}) \tag{3}$$

where $\boldsymbol{\alpha}(\boldsymbol{\theta})$ represents the displacement angle and $\hat{\boldsymbol{\alpha}}(\theta)$ is the Einstein deflection angle derived in the weak gravitational field approximation (see eqn (1) for the case of a point mass). For an extended lens and within the thin lens approximation, we may simply calculate the effective deflection angle by just summing up all individual deflections due to the projection onto the lens plane of (point) mass elements constituting the lens. Although eqn (3) was originally derived for a static

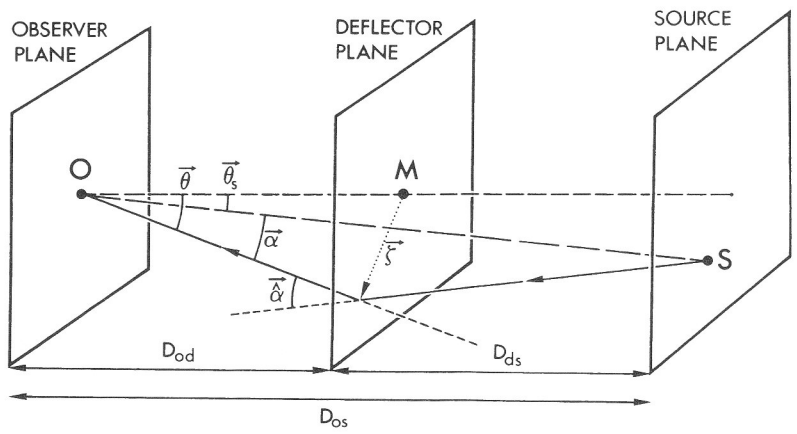


**Figure 4** The deflection of a light ray between a source S and an observer O produced by an intervening point-mass lens (M). (For the other quantities, see the text.)

Euclidian space, Refsdal (1966a) showed that it is also valid for Friedmann–Lemaître–Robertson–Walker (FLRW) expanding universe models provided that $D_{os}$, $D_{od}$ and $D_{ds}$ represent the 'angular size distances' between the observer and the source, the observer and the deflector and the deflector and the source, respectively (e.g. Kayser *et al.* 1997).

We note that a given image position $\boldsymbol{\theta}$ always corresponds to a specific source position $\boldsymbol{\theta}_s$, whereas a given source position $\boldsymbol{\theta}_s$ may sometimes correspond to several distinct image positions $\boldsymbol{\theta}$. Such cases of multiply-imaged sources constitute the most spectacular and interesting aspect of gravitational lensing.

A typical lens situation is shown in Figure 5, where we have projected onto the plane of the sky the true (but invisible) source position and the resulting apparent image positions (two images in this case). We see again that the image position $\boldsymbol{\theta}_i$ is shifted by $\boldsymbol{\alpha}(\boldsymbol{\theta}_i)$ relative to the true source position $\boldsymbol{\theta}_s$; note that $\boldsymbol{\alpha}(\boldsymbol{\theta}_i)$ is usually not constant over an extended lensed image.

Furthermore, Etherington (1933) demonstrated that the specific intensity (or surface brightness) of a light bundle is preserved in curved spaces. Therefore, if the lens is transparent the surface brightness of each lensed image is identical to that of the source, and the resulting amplification is equal to the ratio of the geometrical magnification of the angular size of the corresponding lensed image (e.g. the solid angle subtended by the 'Chwolson' ring) to that of the (unlensed) source. Generally speaking, this magnification $\mu_i$ is thus given by the ratio between the solid angle $d\omega_i$ covered by the lensed image and that of the source $d\omega_s$. In a more formal way, the expression of $\mu_i$ is given for an infinitesimal source by the inverse Jacobian of the transformation between the source and the image planes:

$$\mu_i = \frac{d\omega_i}{d\omega_s} = \left| \det\left(\frac{\partial \boldsymbol{\theta}_s}{\partial \boldsymbol{\theta}_i}\right) \right|^{-1} \tag{4}$$

If a gravitational lens system is composed of several spatially unresolved images, the total magnification (or amplification) is naturally given by the sum of all individual image magnifications (amplifications).

Finally, since the gravitational lensing amplification may vary over the image of an extended source, and if the latter has a shape that is wavelength dependent, then chromatic effects between the different lensed images can result (note the differently magnified source regions in Figure 5), without contravening the achromatic property stipulated earlier for gravitational lensing (eqn (1)). Furthermore, we shall see in Section 3 how multi-waveband observations of such resolved lensed images may enable us to set very helpful constraints on the lens mass distribution and on the source structure itself.

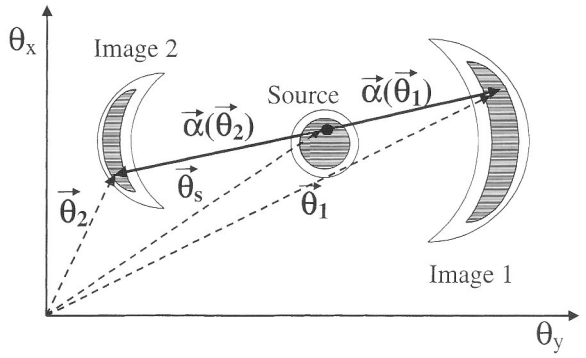


**Figure 5** Images of a doubly imaged source as seen projected onto the sky. The white and darker regions represent different emitting areas as seen at two different wavelengths.

## 2.2 The angular size of the Einstein ring and the condition for multiple imaging

The perfect alignment between the observer, a compact lens characterized by a symmetric mass distribution $M(\xi)$ ($M(\xi)$ representing the mass located within the impact parameter $\xi$, within the distance of minimum approach between the light ray and the lens) and the source corresponds to $\boldsymbol{\theta}_s = \mathbf{0}$ (Figure 4). It is clear in this axially symmetric case that the observer will actually see a ring (the so-called Einstein ring) of light from a distant source (Figure 6). It is possible to show, for an axially symmetric mass distribution, that the deflection vector angle $\hat{\boldsymbol{\alpha}}(\boldsymbol{\theta})$ reduces itself to the scalar angle (compare with eqn (1))

$$\hat{\alpha}(\xi) = \frac{4G}{c^2}\frac{M(\xi)}{\xi} \tag{5}$$

Combining this deflection angle and the lens equation (eqn (3)) for $\theta_s = 0$, the angular radius $\theta_E$ of this Einstein ring may be expressed conveniently as

$$\theta_E = \sqrt{\left(\frac{4GM(D_{od}\,\theta_E)D_{ds}}{c^2 D_{od} D_{os}}\right)} \tag{6}$$

where $M(D_{od}\ \theta_E)$ stands for a mass producing an Einstein ring with radius $\theta_E$, if located at the distance $D_{od}$. $D_{od}$ represents the distance between the observer and the deflector. Note that when expressing the distances appearing in eqn (6) in terms of the source and lens redshifts, the quantity $D_{ds}/(D_{od}\,D_{os})$ is found to be directly proportional to $H_0$.

Listed in Table 1 are typical values of $\theta_E$ for different types of deflectors located at various distances, assuming that the distance between the source and the observer is approximately twice that between the deflector and the observer. We see from Table 1 that for a source and a lens located at cosmological distances ($D_{od} \sim 10^9$ pc), the angle $\theta_E$ can vary from micro-arcseconds (stellar deflection) to arcsecond

(galaxy lensing) scales, and even tens of arcseconds for galaxy cluster lenses.

When there is imperfect alignment between the source, deflector and observer, and for lens mass distributions significantly departing from axial symmetry, the angular separation between multiple lensed images is still about $2\theta_E$, so that eqn (6) may still be used to infer the value of $M/D_{od}$, or the value of $M$ times the Hubble constant $H_0$, if the redshift $z_d$ of the lens and the redshift $z_s$ of the source are known (Section 3.4.2).

By means of eqn (6) we may estimate the average surface mass density of the lens within the Einstein ring. We find that

$$\Sigma_c = \frac{c^2 D_{os}}{4\pi G D_{od} D_{ds}} \tag{7}$$

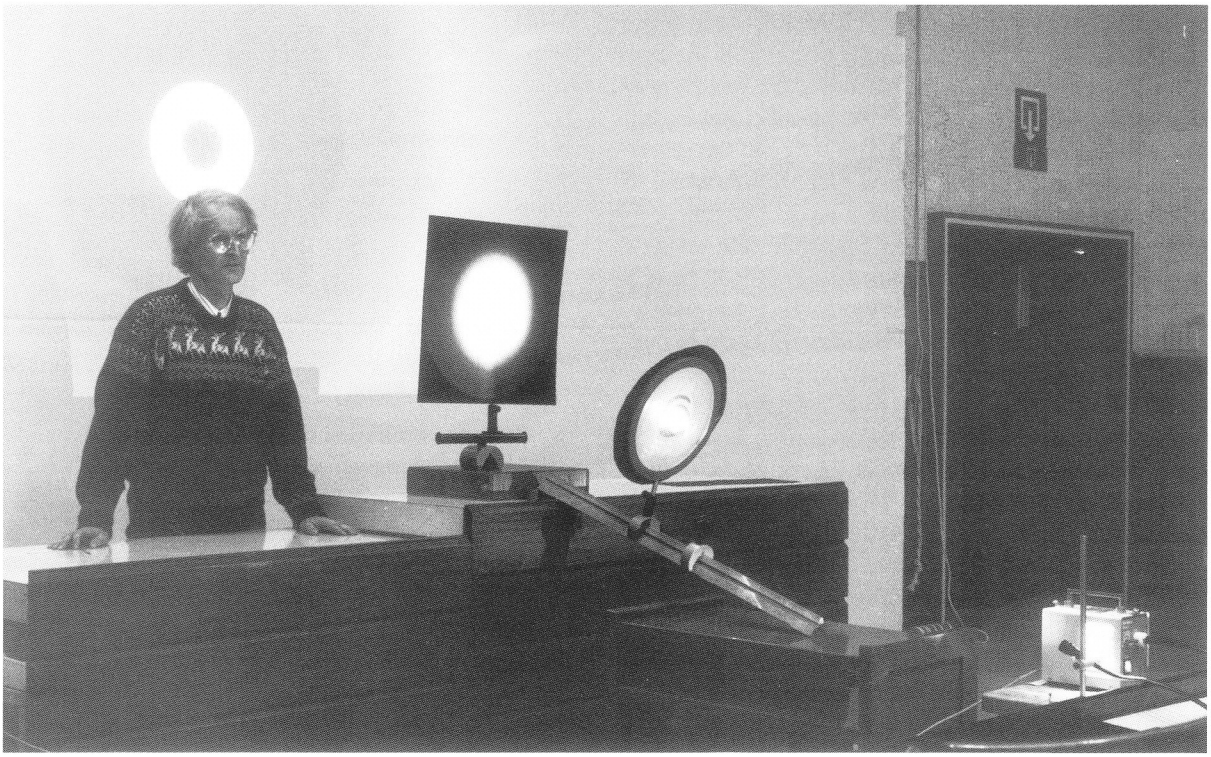

**Figure 6** The gravitational lens experiment. When the observer (the pinhole screen visible in this photograph), a symmetric lens (made of Plexiglas, middle right) and a source (light bulb at bottom right) are in perfect alignment, the observer sees an Einstein ring. The simulation of such a ring is seen here projected onto the background screen during an optical experiment prepared by Professor Sjur Refsdal (seen in this photograph) and one of the authors.

**Table 1** Angular radius ($\theta_E$) of the Einstein ring produced by a deflector with mass $M$ and linear radius $R$ located at a distance $D_{od}$ and a source at a distance $D_{os} = 2D_{od}$. The quantity $\Sigma(R)/\Sigma_c$ represents the ratio between the average ($\Sigma(R)$) and critical ($\Sigma_c$) surface mass densities of the lens (see text).

| Deflectors | Mass ($M_\odot$) | Radius (pc) | $D_{od}$ (pc) | $\theta_E('')$ | $\Sigma(R)/\Sigma_c$ |
|---|---|---|---|---|---|
| Solar planets | $10^{-6}$–$10^{-3}$ | $10^{-10}$–$10^{-9}$ | $10^{-6}$–$10^{-3}$ | $2 \times 10^{-3}$–2 | $< 3\ 10^{-4}$ |
| Exoplanets | $10^{-6}$–$10^{-3}$ | $10^{-10}$–$10^{-9}$ | 1–10 | $2 \times 10^{-5}$–$2 \times 10^{-3}$ | 100–$10^5$ |
| Nearby stars | 1–10 | $10^{-8}$–$10^{-6}$ | 1–100 | $6 \times 10^{-3}$–0.2 | 0.1–$10^6$ |
| Extragalactic stars | 1–10 | $10^{-8}$–$10^{-6}$ | $10^6$–$10^9$ | $2 \times 10^{-6}$–$2 \times 10^{-4}$ | $10^5$–$10^{13}$ |
| Globular clusters | $10^5$ | 1–10 | $10^3$–$10^5$ | $6 \times 10^{-2}$–0.6 | $10^{-7}$–$10^{-3}$ |
| Local galaxies | $10^{10}$–$10^{12}$ | $10^3$–$10^4$ | $10^6$–$10^7$ | 2–64 | $10^{-5}$–1 |
| Distant galaxies | $10^{10}$–$10^{12}$ | $10^3$–$10^4$ | $10^8$–$10^9$ | 0.2–6.4 | $10^{-3}$–100 |
| Galaxy clusters | $10^{14}$–$10^{15}$ | $10^5$–$10^6$ | $10^8$–$10^9$ | 20–200 | $10^{-3}$–10 |

irrespective of the mass distribution of the lens. This average surface mass density $\Sigma_c$ is known in the literature as the critical surface mass density, which depends only on the angular distances between the observer, the lens and the source.

We conclude that the diameter of an Einstein ring adapts itself in such a way that the average surface mass density of the lens inside the ring is always equal to the critical surface mass density $\Sigma_c$. It is then straightforward to understand that a sufficient condition for an observer to see a ring, or multiple images, from a distant source is that, somewhere in the lens plane, the surface mass density $\Sigma$ should exceed the critical value $\Sigma_c$, that is $\Sigma \geqslant \Sigma_c$. On the contrary, if we have $\Sigma < \Sigma_c$ everywhere over the lens, then the object is not capable of forming a cosmic mirage. Given typical cosmological distances for the deflector (redshift $z_d \sim 0.5$) and the source ($z_s \sim 2$), $\Sigma_c \sim 1\,\mathrm{g\,cm^{-2}}$ is found to be roughly equivalent to the surface mass density of a 1 cm thick layer of water.

The average surface mass density for a deflector having a typical mass $M$ and radius $R$ is defined as $\Sigma(R) = M/(\pi R^2)$. Listed in Table 1 are values of the ratio $\Sigma(R)/\Sigma_c$ for planets, stars, globular clusters, galaxies and galaxy clusters as possible deflectors. Note that for an axially symmetric lens, the condition $\Sigma(R) \geqslant \Sigma_c$ is equivalent to the condition $\theta_R \leqslant \theta_E$, $\theta_R$ ($=R/D_{od}$) being the angular radius of the lens, which automatically ensures that the angular extent of the deflector never covers the lensed images typically separated by an angular distance $2\theta_E$ (actually, $\Sigma(R)/\Sigma_c = (\theta_E/\theta_R)^2$).

We may summarize the important information contained in Table 1 as follows. Because their angular sizes are too large as viewed from the Earth, the solar planets are not capable of producing multiple images of background stars. Depending on the angular resolution of the observations, a slight angular shift of the positions of nearby background stars might, however, be detectable. Exoplanets are found to be excellent gravitational lenses ($\Sigma(R)/\Sigma_c \geqslant 1$) and this explains why several teams of astrophysicists are currently involved in searching for rapid light fluctuations induced by planet-like objects in the light-curves of selected stars (Section 3.3). All nearby and extragalactic stars turn out to be very good potential gravitational lenses. Globular clusters and local galaxies are not sufficiently compact to produce cosmic mirages. Finally, very compact, massive galaxies and/or galaxy clusters located at cosmological distances, for which $\Sigma(R)/\Sigma_c \geqslant 1$, constitute promising 'multiple imaging' deflectors.

### 2.3 Axially symmetric lens models

In axially symmetric lens models the propagation of light rays reduces to a one-dimensional problem (see eqns (5) and (6)), and the general lens equation (eqn (3)) transforms into the scalar equation

$$\theta^2 - \theta\,\theta_s - \theta_E^2 \frac{M(D_{od}\,\theta)}{M(D_{od}\,\theta_E)} = 0 \tag{8}$$

The amplification $\mu$ of the lensed images (eqn (4)) is then found to be

$$\mu = \frac{\theta\,\mathrm{d}\theta}{\theta_s\,\mathrm{d}\theta_s} \tag{9}$$

For the point-mass lens model, we have $M(\xi) = M$, and eqn (8) reduces to a second-degree equation in $\theta$ whose solutions are ($i = 1, 2$)

$$\theta_{1,2} = \frac{1}{2}\theta_s \pm \sqrt{\left(\left(\frac{1}{2}\theta_s\right)^2 + \theta_E^2\right)} \tag{10}$$

and the image amplification is given by

$$\mu_i = \frac{1}{1 - (\theta_E/\theta_i)^4} \tag{11}$$

a negative value of $\mu_i$ indicating that the corresponding lensed image is reversed. The positions of the lensed images being given by eqn (10), the total amplification $\mu_T = \mu_1 + |\mu_2|$ of the source can be found for a given value of $\theta_s$:

$$\mu_T = \frac{\theta_s^2 + 2\theta_E^2}{\theta_s \sqrt{(\theta_s^2 + 4\theta_E^2)}} \tag{12}$$

In particular, we find that when the true position of the source lies inside the imaginary Einstein ring (for $\theta_s \leqslant \theta_E$), the total magnification $\mu_T$ of the two images is larger than 1.34. This implies that the cross-section for significant lensing, by convention $\mu_T \geqslant 1.34$, is equal to $\pi\theta_E^2$, which is proportional to the mass $M$ (eqn (6)). We make use of this result when discussing the optical depth for lensing in Section 2.6 and when deriving the expected frequency of multiply-imaged sources to set upper limits on the cosmological density $\Omega_L$ of compact objects in the Universe (Section 3.4.2).

When source, lens and observer are in perfect alignment, the observer sees a ring of light due to the axial symmetry (Section 2.2). Figure 6 illustrates a gravitational lens experiment in which a point-mass optical lens, actually made of Plexiglas, reproduces the deflection of light rays by a black hole having one-third of the Earth's mass (the foot of a wine glass may be used as an acceptable lens simulator). In this experiment, a compact light source (representing e.g. a distant quasar) is located on the right-hand side of the photograph. On the left-hand side of the lens is a white screen with a small hole at the centre (a pinhole screen). Further behind, there is a large screen onto which is projected the lensed image(s) of the source (an Einstein ring in this case) as it would be seen if our eyes were located at the position of the pinhole.

Representative examples of simulated lensed images are illustrated in Figure 7. First, the pinhole is set very precisely on the optical axis of the point-mass lens (Figure 7a, see also Figure 6) so that the source, the lens and the observer (the pinhole) are perfectly aligned. As the pinhole is moved slightly away from the axis of symmetry (Figure 7b), the Einstein ring (slightly elliptical in Figure 7h because of projection effects) breaks into two images (Figure 7i), in accordance with eqns (10) and (11). Note that, due to the point-mass lens used in the optical experiment, the distribution of light across the pinhole screen is not uniform: there is a maximum concentration of light near the optical axis. Thus, the maximum amplification is obtained when the pinhole is very precisely set on the optical axis (Figure 7a), corresponding to the formation of an Einstein ring (Figure 7h). Farther from the centre (Figure 7b) the light gets dimmer; the distribution of light does in fact correspond to convergence points due to pairs of light rays deflected by the lens, and the total amplification of the corresponding images tends towards unity with increasing distance from the axis of symmetry. Figures 7o and 7p illustrate corresponding examples of extragalactic multiply-imaged sources. Some of the images shown in Figure 7 were obtained by the WFPC2 (Figures 7p, 7s, 7t) and NICMOS (Figure 7r) cameras aboard the Hubble Space Telescope (HST).

## 2.4 Asymmetric lens models

As we may expect, symmetric lenses seldom occur in nature; usually the main lens itself is non-symmetric, or some non-symmetric disturbances are induced by the presence of neighbouring masses. In our optical gravitational lens experiment, the effects of a typical non-symmetric (singular) gravitational lens may be simulated by simply tilting the optical lens. The bright focal line along the optical axis in the symmetric configuration (Figure 7a) then becomes a two-dimensional envelope, called a caustic in optics. A section of this caustic is visible as a closed curve having a diamond shape (made of four folds and four cusps) in the pinhole plane (Figures 7c–g). The word 'caustic' in gravitational lensing always refers to this section of the optical two-dimensional caustic (in the symmetric case, the caustic degenerates into a single point, Figure 7a). As a result, the Einstein ring that was observed in the symmetric case (Figure 7h) is now split into four lensed images (Figure 7j). Similar observed examples of gravitational lenses are the multiply-imaged quasars Q2237 + 0305 (known as the Einstein Cross) and H1413 + 117 (the Clover-Leaf; Figure 7q). Such a configuration of four lensed images always arises when the pinhole (observer) is located inside the diamond formed by the caustic.

Figure 7k shows the merging of two of the four images into a single bright image when the pinhole approaches one of the fold caustics (Figure 7d). Some well-known multiply-imaged quasars showing similar image configurations are PG1115 + 080 (the 'triple quasar') and MG0414 + 0534 (the 'dusty lens'). Figure 7r is a direct image of PG1115 + 080 obtained in the near-infrared with the NICMOS camera aboard HST.

Just after the pinhole has passed the fold caustic (Figure 7e), the two merging images totally disappear (Figure 7l). Such a doubly imaged quasar is HE1104-1805 (Figure 7s).

A particularly interesting case occurs when the pinhole (observer) is located very close to one of the cusps (Figure 7f). Three of the four previous lensed images have then merged into one luminous arc, whereas the fourth one appears as a faint counter-image (Figure 7m). Famous luminous arcs have been identified among rich galaxy clusters such as Cl2244−02 and Abell 370 (Figure 7t).

For large sources that cover most of the diamond-shaped caustic (Figure 7g), an almost complete Einstein ring is observed (Figure 7n), although the source, lens and observer are not perfectly aligned and the lens is still tilted. In this last experiment, the increase of the source size has been simulated by significantly enlarging the pinhole radius. Several radio Einstein rings of this sort have been discovered, among them MG1131 + 0456 (Figure 7u) and MG1654 + 1346.

As previously stated, all image configurations illustrated in Figures 7h–n are found among observed gravitational lens systems (Figures 7o–u). If our optical lens had been non-singular in the centre, we would have seen an additional image formed in the central part of the lens. Burke (1981) has in fact demonstrated that a non-singular, transparent (symmetric or asymmetric) lens always produces an odd number of images for a given point source (except when located on a caustic). However, for a singular lens, as in our optical lens experiment, one may obtain an even number of images.

For the known gravitational lenses with an even number of observed images, it may well be that a black hole resides at the centre of the lens. The presence of a compact core could also account for the 'missing' image since the very faint image expected to be seen close to, or through, the core would then be well below the detection limits that are currently achievable. Whereas the formation of multiply-lensed images by non-symmetric gravitational lenses is mathematically well understood (see the pioneering work by Bourassa *et al.* (1973)), the theoretical developments turn out to be very technical and rather tedious. The main results are found to be in very good agreement with the observations simulated in the above optical gravitational lens experiment.

## 2.5 Propagation of a distorted wavefront and time delays

It is interesting that gravitational fields in the Universe deflect electromagnetic waves in a way similar to the bending of light rays in the Earth's atmosphere. Indeed, as mentioned in

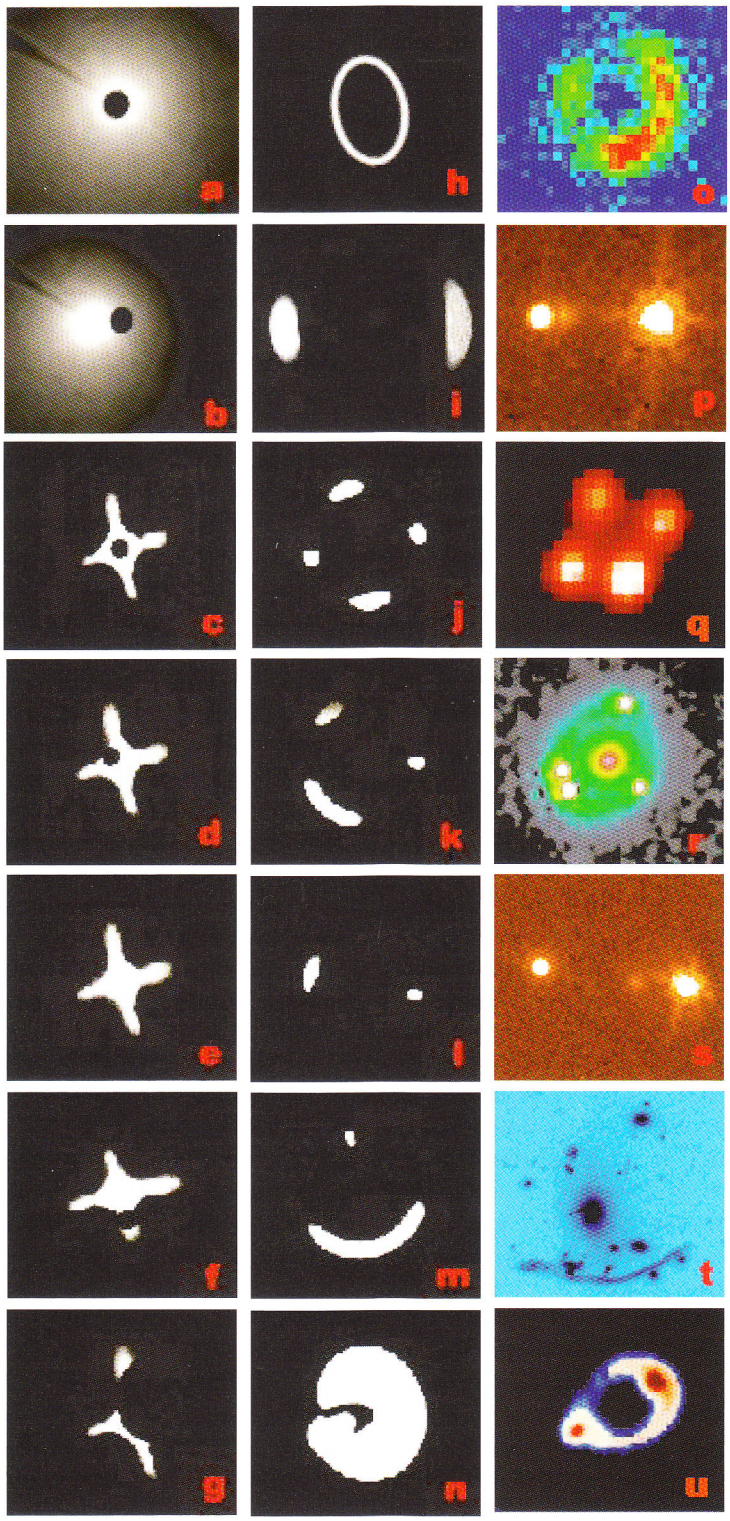


**Figure 7** Images in the left-hand column represent the light from a distant source that is redistributed over the pinhole screen (in the experiment shown in Figure 6) by a symmetric (a, b) or a non-symmetric (c–g) optical lens and for various positions of the pinhole (observer). The central column (h–n) illustrates the corresponding lensed images projected onto the large screen located behind the pinhole screen, and the right-hand column (o–u) displays known examples of multiply-imaged sources (0047−28078, 1009−0252, H1413+117, PG1115+080, HE1104−1805, Abell 370 and MG1131+0456). Images (p), (r), (s) and (t) were obtained by the Hubble Space Telescope, and the others by ground-based facilities (ESO and VLA/NRAO). Courtesy of the European Southern Observatory (ESO), the Space Telescope Science Institute (STScI) operated for NASA by AURA, and the Very Large Array (National Radio Astronomy Observatory).

Section 1, we may associate with any point in space an equivalent refractive index $n$ that is entirely defined by the Newtonian potential $U$ of a given deflector (eqn (2)). For the particular case of a deflector characterized by a density distribution of the type $\rho(r) = \rho_0 \exp(-r/r_c)$, $r_c$ being a scaling factor, Figure 8 illustrates the propagation of light rays and of successive wavefronts from a distant source. Close to the source the wavefronts are spherical, but as they approach the lens they become deformed by curvature effects and time retardation ($v = c/n$) and can, in many

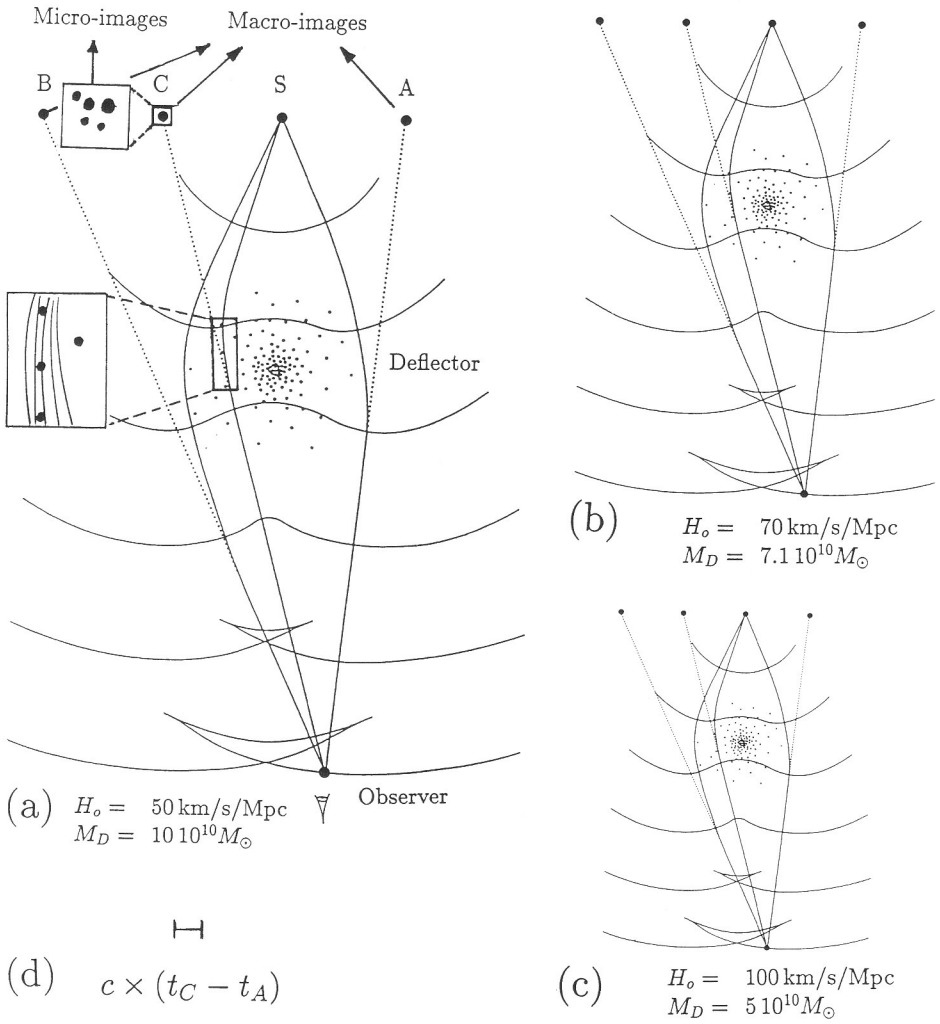


**Figure 8** (a) Propagation of light rays and of corresponding wavefronts from a distant source near a deflector characterized by an exponential volume density distribution (see the text). For different values (50, 70 and 100 km $s^{-1}$ $Mpc^{-1}$) of the Hubble constant $H_0$ and corresponding values for the deflecting mass $M$ (such that $M H_0 = \text{const.}$, see eqn (6) and the note just below), (a), (b) and (c) represent the scaled versions of a gravitational lens system as seen by an observer under a similar angular configuration (all angles measured by the observer on the plane of the sky between the macro-lensed images and the deflector are the same). Given the length of the segment $c\,(t_C - t_A)$ represented in (d), where $c$ is the velocity of light and $t_C - t_A$ is the observed time delay between the lensed images C and A, it is straightforward to conclude that only one of the proposed models (namely model (b)) is compatible with the measured delay $t_C - t_A$ between the arrival times of the corresponding wavefronts at the observer (compare the length of the segment in (d) with the path differences in (a), (b) and (c) between the wavefronts for images A and C). This is the principle of the method first proposed by Refsdal (1964b) to determine the value of $H_0$ from the measurement of the time delay. In (a) we have also represented the splitting of macro-image C into several micro-images, with typical angular separations of approximately one micro-arc second, due to gravitational lensing by individual stars located along its line of sight.

cases, self-intersect. This self-intersection is directly related to the formation of multiple images since each crossing of the wavefront at the observer corresponds to the formation of an image in the direction perpendicular to the local wavefront. Note in Figure 8 the complex shape of the distorted wavefront after crossing the deflector plane. In this case, up to three successive parts of a single-folded wavefront (i.e. up to three distinct light rays) can reach an observer, leading to the formation of up to three distinct lensed images. Of course, due to the different geometric lengths of these light trajectories and to the apparently varying speed of light across the deflector, these different parts of a same wavefront reach the observer with time delays. Refsdal (1964b, 1966a) has shown that if it is possible to model the observations of a gravitational lens system successfully, it is straightforward to derive the distance scale of the Universe, or equivalently the value of the Hubble constant $H_0$, from the measurement of the time delay between a single photometric event detected at two different epochs in the light-curves of two lensed images (Figures 8a, b and c; see Section 3.4.2 for more details).

## 2.6 Gravitational lensing optical depth

If some luminous sources are *a priori* more likely to be lensed than others, then seeking them out should reveal new cosmic mirages.

Let us assume for simplicity a non-evolving population of lenses with mass $M$, whose co-moving space density is thus a constant, $n_0(M)$. The optical depth $\tau$ for lensing a source located at redshift $z_s$ is then

$$\tau(z_s, M) = V_{\rm eff}(z_s, M)\, n_0(M) \tag{13}$$

where $V_{\rm eff}$ represents the co-moving volume in which the lens must be located in order to produce an *observable* gravitational mirage (Nemiroff 1989). 'Observable' here means that the angular separation and the magnitude difference between the multiply-lensed images can be resolved with the instrument used for the observations. $V_{\rm eff}$ simply results from the integration of the effective cross-section $\Sigma_{\rm eff}$ along the line of sight:

$$V_{\rm eff}(z_s, M) = \int_0^{z_s} (1+z)^3 \Sigma_{\rm eff}(z, M; z_s, p_i) \frac{c\,{\rm d}t}{{\rm d}z} {\rm d}z \tag{14}$$

where $p_i$ are the lens parameters.

For Friedmann–Lemaître–Robertson–Walker cosmologies, the line-of-sight derivative element $c{\rm d}t/{\rm d}z$ is given as a function of the present matter density $\Omega_0$ and the cosmological constant $\lambda_0$ by the following relation (e.g. Kayser *et al.* 1997):

$$\frac{c\,{\rm d}t}{{\rm d}z} = \frac{c}{H_0\sqrt{(1+z)}} \times \frac{1}{\sqrt{\left[(1+z)^3\Omega_0 - (1+z)^2(\Omega_0 + \lambda_0 - 1) + \lambda_0\right]}} \tag{15}$$

For a point-mass lens, we have seen in Section 2.3 that a typical cross-section for significant gravitational lensing is defined as $\Sigma_{\rm eff} = \pi\theta_{\rm E}^2$. Such a cross-section may be generalized for any other type of deflector (e.g. a galaxy lens model). Rigorously, it should of course take into account the limited angular resolution and dynamic range of the instrument used to perform the observations. Given eqns (6) and (15), we see that the expression of the optical depth defined in eqn (13) is independent of the Hubble constant $H_0$.

The total flux coming from multiply-lensed images is always amplified by a certain factor $\mu_{\rm T}$ with respect to the source flux (Section 2.3). Therefore the probability that a source with redshift $z_s$ and apparent magnitude $b_s$ is a lensed object is not simply $\tau(z_s, M)$, but is given by

$$\begin{aligned} P(z_s, b_s) &= \frac{N_{\rm L}(z_s, b_s)}{N_s(z_s, b_s)} \\ &= \frac{\tau(z_s) N_s(z_s, b_s + 2.5\log\mu_{\rm T})}{N_s(z_s, b_s)} \\ &= \tau(z_s){\rm Bias}\,(z_s, b_s) \end{aligned} \tag{16}$$

where the number–magnitude relations $N_{\rm L}(z_s, b_s)$ and $N_s(z_s, b_s)$ represent respectively the number of multiply-imaged sources and unlensed sources at redshift $z_s$ and blue magnitude $b_s$ per square degree and per magnitude interval; the last equality defines the so-called amplification bias.

Faint sources are usually, more numerous than bright ones, so the amplification bias is quite often larger than 1. Moreover, if the number counts of sources increase faster at bright magnitudes, the corresponding proportion of mirages becomes larger. Therefore, eqns (13) and (16) show that the most likely lensed sources are (1) distant ($V_{\rm eff}$ is maximized) and (2) bright objects belonging to a population with a steep number–magnitude relation at the observed wavelength (the amplification bias is then high; Turner 1980).

Highly luminous quasars (HLQs; typically $M_{\rm V} \leqslant -27.5$ for $H_0 = 50\,{\rm km\,s^{-1}\ Mpc^{-1}}$) have long been recognized as excellent targets to search for new gravitational lenses because they are both distant and bright sources (Turner *et al.* 1984, Surdej *et al.* 1988). Their number–magnitude relation has a steep bright end with a break around the apparent magnitude $b = 19.2$ (Boyle *et al.* 1988, Hartwick and Schade 1990). They have been selected for search for gravitational

lenses by several teams; successful results are presented in Section 3.

## 3 ASTROPHYSICAL AND COSMOLOGICAL APPLICATIONS

### 3.1 Introduction

In this section we show how it has been possible to derive unique information on the deflecting objects, on the sources themselves and on the Universe as a whole from the observations and studies of distorted and/or multiple images of distant lensed objects. We look at some of the most important astrophysical and cosmological applications of gravitational lensing with respect to the distance of the lens, going from the Solar System to distant quasars and the very edge of the Universe. During this tour, we shall discover how the disturbing effects of lensing can be transformed into tools to improve our knowledge of the Universe. We also indicate how space observations have helped to establish some of these results.

### 3.2 Light deflection in the Solar System

Starting our trip from Earth, the closest lens is actually the Earth's atmosphere itself. The refraction of light rays coming from space in the denser layers of the atmosphere slightly changes the apparent positions of stars on the sky. In order to precisely point a telescope towards a given star, corrections for refraction are required. This phenomenon is more pronounced when a star is close to the horizon: a particular example is the deformation of the Sun's image at sunset. Sometimes, multiple images of the Sun can be seen, resulting in the formation of a mirage. Refraction must also be taken into account when the length of the light path in the atmosphere must be precisely known, for example in the context of atmospheric chemistry, either performed from the ground or from spacecraft.

As seen from Earth, gravitational light deflection in the Solar System does not lead to the formation of multiple images of background sources because the apparent size of the deflectors (the Sun or the planets) is larger than their angular Einstein radius (Section 2.2). However, the measurement of the change of the apparent positions of background sources located near the line of sight to the Sun or to Jupiter are very important from the point of view of fundamental physics. We have already seen that the shift in the positions of stars located close to the limb of the Sun observed by Eddington and his collaborators during the total eclipse of 1919 secured the second experimental confirmation of the theory of general relativity. At that time, the relatively poor accuracy (20–30% uncertainty) of the observations was nevertheless just sufficient to distinguish between Newton's prediction and that of Einstein. Thanks to radio interferometric observations of quasi-stellar sources carried out with the VLA, VLBI or VLBA (Fomalont and Sramek 1975a,b; Robertson *et al.* 1991; Lebach *et al.* 1995), it has been possible to measure the gravitational deflection of radio waves by the Sun with uncertainties much less than 1%. Because of these high accuracies, selecting among the alternative theories of gravitation has now become feasible (Robertson *et al.* 1991). General relativity still seems to be preferred. The measurements of the bending of light rays near the Sun at both optical and radio wavelengths do actually constitute the first multi-waveband observations of 'gravitational lensing', verifying at the same time the expected 'achromaticity' of the phenomenon (eqn (1)).

The apparent displacement of the radio source P0201 + 113 by 300 micro-arcseconds due to a close alignment with Jupiter has also been qualitatively measured (Treuhaft and Lowe 1991). Finally, let us note that the light coming from a star located at 90° from the Sun still undergoes a deflection of 4 milli-arcseconds. Therefore the revolution of the Earth around the Sun induces a tiny, annual astrometric shift for all stars in the sky. This has been confirmed with the Hipparcos satellite (Froeschlé *et al.* 1997). The measurements by the ESA Cornerstone mission GAIA (Global Astrometric Interferometer for Astrophysics, now the Galactic Census Project) should be much more sensitive to the influence of the massive planets Jupiter and Saturn, and will improve the constraint on the alternative theories of gravity by several orders of magnitude (Section 4.1). For more details, see Chapter 15.

### 3.3 Microlensing in the Milky Way

In order to produce multiple images of a distant star with an angular separation larger than its physical diameter, a deflector like the Sun should be located at a distance from Earth larger than typically 550 AU, or 0.01 light years. This is more than 10 times the size of the Solar System (as defined by Neptune's orbit). So, we are now in our Galaxy. One of the nearest stars, $\alpha$ Centauri, is at a distance of approximately 4.3 light years. If it were used as a deflector, the expected angular separation between the lensed images of background stars would be only about 0.2 arcseconds, and the misalignment should be no worse than about 0.1 arcseconds, otherwise the secondary lensed image will be too faint to be detectable (Section 2.3, eqn (11)), especially in the glare of the foreground star. And the more distant the deflecting star, the smaller the angular separation between the lensed images of background sources, which then falls below the resolution of conventional instruments (eqn (6)). We then talk of *microlensing*. (This is probably why Einstein was so pessimistic about the possibility of observing gravitational lensing among stars.)

However, in an important paper Paczyński (1986) put forward a point concerning gravitational microlensing in the Milky Way: it can be used either to detect or to rule out dark compact objects as a major constituent of the halo of the Galaxy. In 1991, Griest coined the acronym MACHOs for these massive astrophysical compact halo objects. Indeed, everything moves in the Galaxy, so the relative alignments between background stars and potential unseen deflectors continuously change. When the alignment is good, lensed images cannot be resolved but the increase in the total flux can be recorded (eqn (12)). The probability of having an amplification $\mu_T \geqslant 1.34$ (or the optical depth for microlensing; see Section 2.6) is very small ($10^{-7}$) but this can be compensated for by observing a huge number of stars, located for example in the Magellanic Clouds. The technology was ready for handling such a huge amount of data. Several independent teams (EROS, Expérience de Recherche d'Objets Sombres; MACHO; OGLE, Optical Gravitational Lensing Experiment; and so on) started the ambitious programme of monitoring each night millions of stars located in the Magellanic Clouds, or later towards the galactic centre, waiting for microlensing events – achromatic, symmetric and non-repeating flux variations. The first detections were reported by different groups in 1993, and more than 500 events have been detected so far, mainly towards the galactic bulge (see the review by Paczyński (1996) for further details on the analysis and the first results). Interpreted in the context of microlensing by dark compact objects in the halo of the Milky Way, the current observations of the Large Magellanic Cloud (LMC) imply a MACHO halo fraction of about 20%. The most likely MACHO mass is between $0.15\,M_\odot$ and $0.9\,M_\odot$; the mass range $10^{-7}$–$10^{-2}M_\odot$ is excluded at the 95% confidence level (Aubourg and Palanque-Delabrouille 1999, Alcock *et al.* 2000).

However, the physical nature of MACHOs is not clear yet. For example, if they are white dwarfs, a strong chemical enrichment of the halo should have been observed. But some of the observed events could be caused by lenses located in the LMC itself (self-lensing): degeneracies between the parameters make it impossible to determine independently the distance of a single lens from the analysis of the light-curve. One solution, discussed by Refsdal (1966b), is to take advantage of the parallax effect: basically, two observers separated by a distance $d$ in the observer plane will see the same light-curve but with a time lag $t = d/v$, where $v$ is the apparent speed of the caustic projected in the observer plane along the line connecting them. (With three observers, the unknown orientation of the caustic can be retrieved.) The parallax induced by the revolution of the Earth around the Sun distorts long-duration light-curves. For short ones, simultaneous observations with two spacecraft located a few astronomical units apart should ideally be performed.

Binary lenses produce different kinds of light-curves. This opens the possibility of detecting planets orbiting the star-lens. The light-curves need to be extremely well sampled. They are usually obtained by means of sustained photometric monitoring campaigns mounted when alerts of ongoing microlensing events are made (e.g. the PLANET – Probing Lensing Anomalies NETwork-collaboration, Albrow *et al.* 1998).

### 3.4 Multiply-imaged quasi-stellar objects

Extragalactic gravitational lensing was first mentioned by Zwicky in 1937. He realized that, due to their large mass, external galaxies might lens more distant ones into several *observable* images. However, such mirages are still difficult to identify because galaxies are faint, diffuse and extended objects whose apparent size can be large compared with the Einstein ring of the lens.

In 1963 the first quasar was discovered by Schmidt. Quasars are the beacons of the Universe. Thanks to their huge luminosity, they can be seen at very large distances, so the probability of finding a foreground lensing galaxy close to the line of sight is larger than for normal galaxies. Moreover, multiply-lensed images of quasars can be more easily identified because the source is bright and point-like (Peterson 1997). In 1979, the first cosmic mirage was found by chance as a double image of a radio-loud quasar (Walsh *et al.* 1979), with identical spectral properties from UV (measured with the International Ultraviolet Explorer satellite by Gondhalekar and Wilson in 1980) to radio through optical and infrared wavelengths. This discovery prompted new interest in gravitational lensing. A large number of applications became possible and motivated several independent teams to find more and more gravitational lenses among selected high-luminosity quasars. HLQs are indeed more likely to be lensed because they are distant and apparently bright: their brightness could be partially due to light amplification by gravitational lensing (the so-called amplification bias; see Section 2.6). However, the probability of being lensed is only about 1%, so large samples have to be observed with ground-based optical or radio telescopes.

Due to the arcsecond scale of the angular separation between the lensed images of QSOs, the HST is often needed to confirm the nature of lens candidates. This is illustrated in the case of the doubly imaged QSO J03.13 A and B ($z_s = 2.55$, $\Delta\theta = 0.84''$), which was discovered at the European Southern Observatory, La Silla, Chile (Figure 9a) to be a good lens candidate, then confirmed with HST to consist of two point-like images (Figure 9b) having identical spectra (Figure 9c).

By the end of the century more than 50 multiply-imaged quasars had been identified (see Claeskens and Surdej (2001) for a complete list). Figures 7 and 9b illustrate several representative ones. In the following we present some of

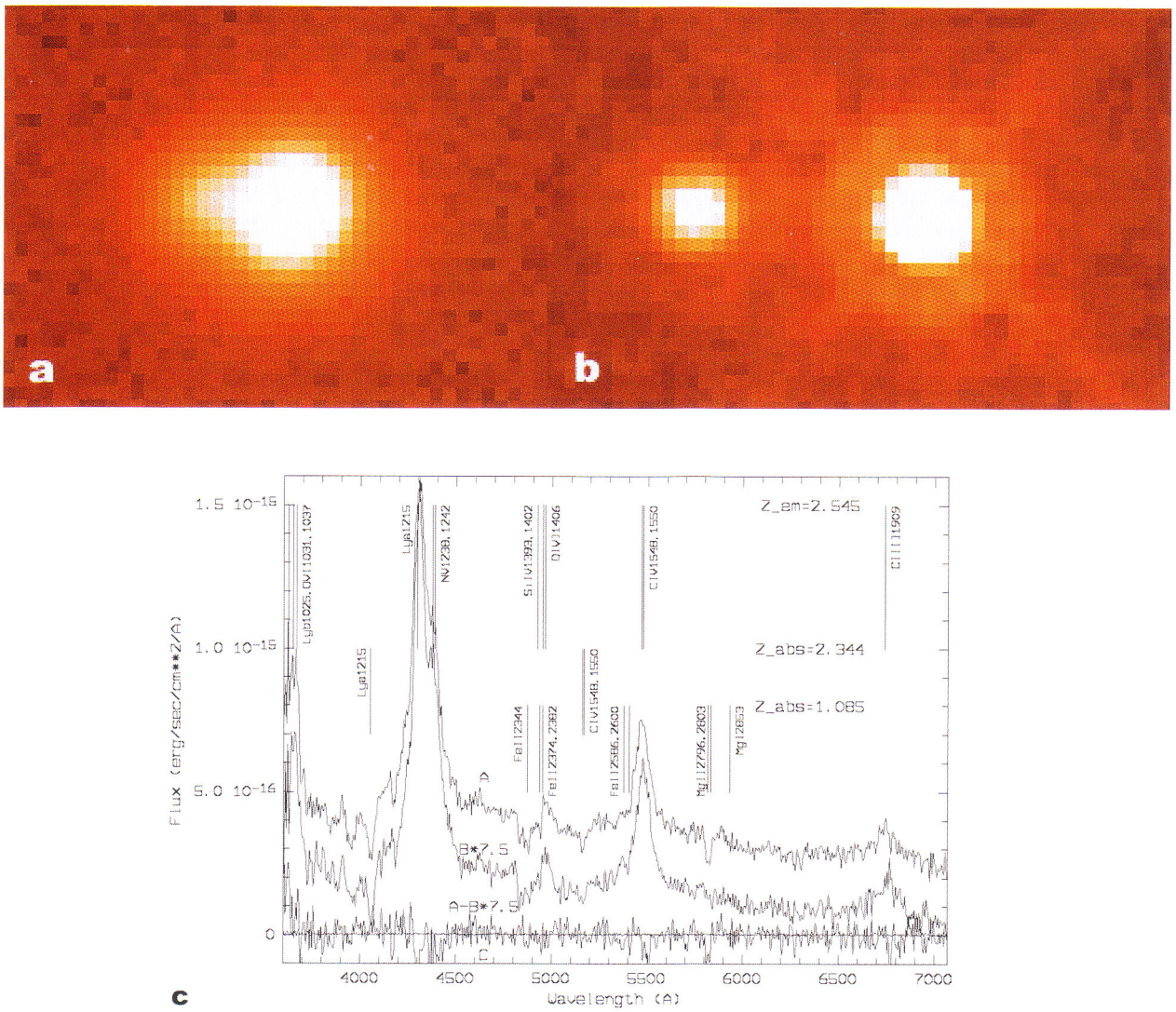


**Figure 9** (a) Identification of a gravitational lens candidate based on ground-based direct CCD imagery. On this CCD frame obtained with the New Technology Telescope (NTT) at La Silla (Chile), the image of the QSO J03.13 looks somewhat elongated. The seeing was about 0.7". Claeskens *et al.* (1996) suspected that J03.13 was composed of two nearby point-like images. (b) Subsequently, the WFPC2 camera abord the HST was used to confirm the image structure of J03.13. This WFPC2 R CCD frame clearly reveals a double image, with an angular separation of 0.84". (c) For such a small angular separation, it is impossible to obtain individual spectra of the resolved components from the ground. This is an easy task, however, for the HST. Spectra obtained with the Faint Object Spectrograph instrument clearly show that the fingerprints of J03.13 A and B cannot be distinguished from each other, except for a few narrow absorption lines due to distinct intervening clouds located along the two lines of sight. These two spectra show that the quasar is at a redshift $z_s = 2.55$ (Surdej *et al.* 1997). (Courtesy of the European Southern Observatory (ESO) and the Space Telescope Science Institute (STScI) operated for NASA by AURA.)

the most interesting applications and results obtained from gravitational lensing effects in quasar samples.

### 3.4.1 *The lensing galaxies*

Multiply-imaged QSOs provide general constraints on the mass distribution of the lensing galaxies. For example, if the value of the Hubble constant $H_0$ and the lens and source redshifts are known, the total mass can be derived from the angular separation between the QSO lensed images, since $\Delta\theta \sim 2\theta_E$ (eqn (6)). This is the simplest and most direct astrophysical application of gravitational lensing.

If a time delay is also measured, the lensing mass can be obtained independently of the cosmological parameters $H_0$,

$\Omega_0$, $\lambda_0$ and the source redshift (Borgeest 1986, Schneider *et al.* 1992). The inferred values for the mass are typical of elliptical galaxies (see Claeskens and Surdej (2001) for a summary of mass and mass-to-light ratio estimates).

Furthermore, the absence of observed cosmic mirages with three images was soon recognized as the signature of nearly singular potentials (Wallington and Narayan 1993; Kochanek 1996), in agreement with HST observations of local elliptical galaxies by Gebhardt *et al.* (1996). Quadruply-imaged quasars can be produced only by asymmetric lenses (Section 2.4; the asymmetry being intrinsic to the lens or due to the perturbing shear of objects located close to the line of sight of the main lens). Generally, the lensed images are better reproduced by lensing isothermal dark matter halos rather than by constant *M/L* lens models (Maoz and Rix 1993; Kochanek 1996). However, the relative positions and flux ratios of the point-like QSO images yield few constraints on the full mass distribution of the lens. This results in degenerated lens models, as first pointed out by Falco *et al.* (1985) and Gorenstein *et al.* (1988), who noted that a given configuration of lensed images can be reproduced with a lighter lensing galaxy inside a galaxy cluster. Thus, additional constraints must be obtained, either from direct observations of the lens environment or from the detection of lensed extended structures, such as the QSO's host galaxy. In the latter case, VLBI or HST high angular resolution is mandatory.

Since the shape and the size of such extended structures may be wavelength dependent, they provide interesting constraints on the mass distribution of the distant deflector and also on the physical modelling of the chromatic structure of the source itself. Existing multi-wavelength observations of multiply-imaged sources, resolved at arcsecond and sub-arcsecond angular scales, have already been successfully inverted. In several cases it has been possible from such analyses to retrieve the mass distribution of the lensing galaxy as well as the multi-wavelength shape of the source (see Wallington *et al.* (1996) for a discussion of the numerical methods, and Claeskens and Surdej (2001) for a general review of the observations). In order to refine such astrophysical applications, it is very important in the future that not only direct imaging but also imaging spectroscopy, at high angular resolution and with a good dynamic range, become feasible at many different wavelengths, both from space (far-UV, X-ray, $\gamma$-ray, near- and mid-infrared, etc.) and from the ground (visible, radio, etc.). An imaging spectroscopy device has been proposed for the Next Generation Space Telescope (NGST). Such an instrument should make it possible to observe very compact gravitational lenses at relatively high angular resolution in the near- and mid-infrared.

The HST plays a crucial role in detecting the main lenses, which are faint, extended high-redshift objects located between bright, small-separation (~1 arcsecond) images of the background quasars. Many lens detections and magnitude measurements have come from the CfA–Arizona Space Telescope LEns Survey (CASTLES), an ongoing HST direct-imaging programme in the H, I and V bands for all the known gravitational lenses as well as published candidates (Muñoz *et al.* 1999a; Figure 7). So far, spectroscopic redshifts of the lenses have been obtained for 52% of the known multiply-imaged QSOs. The median redshift is 0.47, which is exactly where the lenses are the most efficient since the critical surface mass density is expected to be minimum around $z = 0.5$ for high-redshift sources (eqn (7)).

Finally, multiply-imaged quasars need to be investigated carefully in order to determine the extinction law in the lensing galaxies. Indeed, when the lines of sight corresponding to the different images probe different dust optical depths in the lens, a differential reddening is observed between the lensed images. This is the case with, for example, Q2237 + 0305 (Nadeau *et al.* 1991), MG0414 + 0534 (Angonin-Willaime *et al.* 1999) and RXJ0911.4 + 0551 (Burud *et al.* 1998). Jean and Surdej (1998) have refined this technique to estimate the redshift of the lens, whatever its visibility. Until now only galactic parametric curves have been fitted from photometric data, but high-quality spectrophotometry should allow one to determine directly the extinction law at high redshift and compare it with that observed in the Milky Way, in the Magellanic Clouds and in a few local galaxies.

### 3.4.2 *The cosmological parameters*

Extragalactic gravitational lensing provides us with an experiment whose optical bench has a size comparable to that of the observable Universe. Since this size is directly related to the values of the cosmological parameters, it is not surprising that the latter can be constrained from gravitational lensing observations. We refer the reader to Chapter 17 for an extended review of the general determination of the cosmological parameters.

#### The Hubble constant, $H_0$

The Hubble constant fixes the actual expansion rate of the Universe. Its determination from the observation of a multiply-imaged extragalactic source is a very original application of gravitational lensing, proposed in 1964 by Refsdal, and is based on the observation of a time delay between flux variations in the lensed images. The major interest of this method is that it avoids the traditional issue of flux calibrations relying on the difficult-to-prove existence of standard candles, like Type Ia supernovae.

Since the angular separation between multiply-lensed images $\Delta\theta \sim 2\theta_E$ is proportional to $\sqrt{(MH_0)}$ (eqn (6) and the note just below it), a larger deflecting mass combined

with a lower value of $H_0$ produces the same angular separation. However, a lower value of $H_0$ corresponds to larger extragalactic distances and therefore to longer time delays $\Delta t_{i,j}$ between flux variations of two lensed images $i$ and $j$ (Figure 8). More generally, $H_0$ is inversely proportional to the time delay (e.g. Claeskens and Surdej 2001):

$$\Delta t_{i,j} = H_0^{-1}(1 + z_d)\, D(z_d, z_s, \Omega_0, \lambda_0) f(\boldsymbol{\theta}_i, \boldsymbol{\theta}_j, \text{lens model}) \quad (17)$$

where $z_d$ is the redshift of the deflector, $D = D_{od}D_{os}/D_{ds}$ and $f$ is a lens-model-dependent function of the observed image positions $\boldsymbol{\theta}_i$ and $\boldsymbol{\theta}_j$.

Therefore, a successful determination of $H_0$ relies on:

- intensive photometric monitoring of a *variable* multiply-imaged QSO in order to determine precisely $\Delta t_{i,j}$;
- accurate observations of the vector positions $\boldsymbol{\theta}_i$ and $\boldsymbol{\theta}_j$ of the lensed images with respect to the deflector (for example, with HST);
- good knowledge of the lens redshift $z_d$ (the uncertainty due to the lack of accurate values of the other cosmological parameters is negligible as long as the lens redshift is moderate, $z_d \sim 0.5$); and
- a very good estimate of the deflector mass distribution.

As already mentioned in Section 3.4.1, the last item represents the most difficult issue, and complementary observations of the lens and/or the detection of lensed extended structures of the source are required.

Despite the fact that the lens of Q0957 + 561 is complex (denoting the presence of a cluster), it is still probably the best-constrained system, and an accurate value of $\Delta t = 417 \pm 3$ days (Kundić *et al.* 1997; see also Vanderriest *et al.* 1989) has been observed for the time delay. Depending on the actual lens model and constraint set, the results currently range, with errors at $2\sigma$, between $H_0 = 77^{+29}_{-24}$ km s$^{-1}$ Mpc$^{-1}$ (Bernstein and Fischer 1999) and $H_0 = 55^{+15}_{-14}$ km s$^{-1}$ Mpc$^{-1}$ (Chae 1999). Other estimates of $H_0$ are summarized in Claeskens and Surdej (2001).

### The cosmological constant, $\lambda_0$

The fate of the Universe is intimately related to the values of the cosmological density $\Omega_0$ and the cosmological constant $\lambda_0$. Their determination constitutes one of the most important challenges in present-day observational cosmology.

Since the spatial volume of a sphere extending to a given redshift increases for lower values of $\Omega_0$ or for larger values of $\lambda_0$, the resulting number of multiply-imaged QSOs in a large sample of HLQs also increases for such values of the cosmological parameters, assuming the co-moving density of galaxies to be constant; this property was first pointed out by Turner (1990) and Fukugita *et al.* (1990). The influence of $\lambda_0$ is much stronger than that of $\Omega_0$: whatever a reasonable value of $\Omega_0$, values of $\lambda_0$ close to 1 lead to the prediction of detecting at least twice as many lenses than are actually observed in optical samples. Gravitational lensing statistical studies thus place a natural *upper* limit on the value of the cosmological constant, but no significant constraint on $\Omega_0$.

A statistical analysis based on the concept of lensing optical depth (Section 2.6) in an optical sample of 862 HLQs led Kochanek (1996) to the conclusion that $\lambda_0 < 0.66$ at a 95% confidence level (CL), and Claeskens (1999) derived $\lambda_0 < 0.5$ at the same CL from the number of lenses in an optical sample of 1164 HLQs. Similar analyses have also been performed at radio wavelengths with the Jodrell Bank VLA Astrometric Survey (JVAS) of 2500 flat-radio spectrum sources by Falco *et al.* (1998) and by Helbig *et al.* (1999), and with the first part of the Cosmic Lens All Sky Survey (CLASS) by Cooray (1999). They find, respectively, for flat cosmological models, $\lambda_0 < 0.73$, $\lambda_0 < 0.84$ and $\lambda_0 < 0.79$ at 95% CL. Constraints from radio surveys are more compatible with the estimates based on the analysis of high-redshift supernovae (Riess 1998; Perlmutter *et al.* 1999).

Extinguished secondary lensed images or extremely reddened QSOs could remain undetected in optical samples, resulting in incompleteness in the parent QSO sample and affected statistics. Radio surveys are free from such observational dust-obscuration biases, but the distribution of radio sources as a function of their flux and redshift, intervening in the computation of the amplification bias, is not well known. It must be better studied before further improvements on the statistics can be made.

### The cosmological density of dark compact objects

Press and Gunn (1973) noted that counting gravitational lensing events in a sample of distant sources may help in constraining the contribution ($\Omega_L$) to the critical density of the Universe due to a putative cosmological population of dark compact objects with a mass $M_L$ (Section 2.6). Ground-based optical telescopes can reveal the multiple images produced by dark compact objects with a mass $M_L$ between $10^{10.5}$ and $10^{15} M_\odot$. Because of its higher angular resolution, the HST is sensitive to masses down to $10^9 M_\odot$. Radio observations with the VLBI allow one to reach the level of $M_L = 10^6 M_\odot$ (Wilkinson *et al.* 2001). Below that mass range, the lensed images cannot be resolved and constraints come only from the observed statistical variability of the QSO flux or of the equivalent width of their emission lines due to (micro)lensing by the putative dark compact object population (Canizares 1982, Schneider 1993, Dalcanton *et al.* 1994, Nemiroff *et al.* 2001). The available constraints are summarized in Figure 10, and the conclusion is that there is no cosmological population of dark compact objects with mass $M_L$ in the range $10^{-3}$–$10^{13} M_\odot$ capable of closing the Universe.

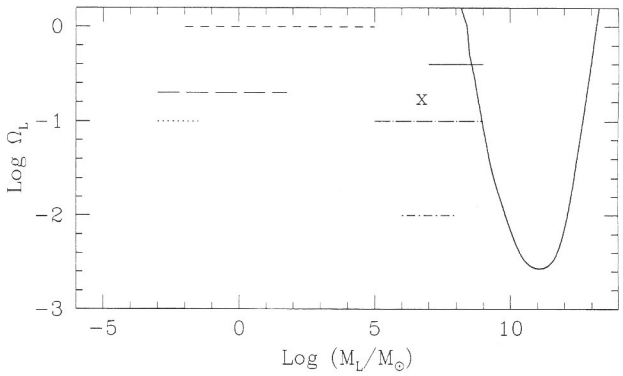


**Figure 10** Current constraints from gravitational lens studies on the cosmological density of dark compact objects (in units of the critical density $\Omega_c$) as a function of their mass. Full curve: Claeskens (1999), 99.7% confidence level ( CL); straight full line: Kassiola *et al.* (1991), 99.7% CL; short-dashed line: Canizares (1982); dotted line: Schneider (1993), ~97% CL; long-dashed line: Dalcanton *et al.* (1994); X: Marani *et al.* (1999), 90% CL; dot–short-dashed line: Wilkinson *et al.* (2001), 95% CL; dot–long-dashed line: Nemiroff *et al.* (2001; ~3$\sigma$).

### 3.4.3 *Size of intergalactic clouds*

Cold intergalactic clouds, which may be connected with galaxy formation (e.g. Wolfe 1988), are revealed by their Lyman α and/or metallic absorption lines (C IV, Mg II, ...) seen in the spectra of distant quasars. If such a distant QSO is multiply-imaged by gravitational lensing, the different lines of sight probe the clouds at various impact parameters. The large number of coincident absorption lines found in the spectra of the multiply-imaged QSOs UM673 A and B (Smette *et al.* 1992) and HE1104-1805 A and B (Smette *et al.* 1995) implies that most of the intervening clouds extend over both lines of sight. A lower limit on their size was derived as 6 and 50 $h^{-1}$ kpc respectively ($h = H_0/100$), in agreement with even larger estimates of about $300h^{-1}$ kpc found from spectroscopic studies of QSO pairs (d'Odorico *et al.* 1998).

### 3.4.4 *Microlensing in multiply-imaged QSOs*

We saw in Section 3.3 that the optical depth for microlensing of a star in the Milky Way by another stellar object is very small. In contrast, since with a multiply-imaged QSO the different lines of sight pass through the halo of the lens, the optical depth for microlensing is much higher, provided the lensing galaxy is made of compact objects (Figure 8a). This was already recognized by Gott (1981). A stellar microlens only quantitatively modifies the flux coming from sources *smaller* than their Einstein radius or smaller than the size of the caustic in the source plane. Thus microlensing preferentially amplifies the continuum emission region, which is the most central part of the QSO (~$10^{-3}$ pc, corresponding to an angular size of $<10^{-6}$″) while the broad emission-line flux (emitting region >1 pc) remains unchanged. Therefore microlensing in multiply-imaged QSOs allows one not only to place limits on MACHOs in external galaxies, but also to constrain the size of the continuum-emitting region of the quasars, which is not directly resolvable with current instruments (e.g. Schmidt and Wambsganss 1998). Recall that QSO structures on larger scales can be studied more easily owing to the 'telescope effect' of the whole lensing galaxy on the macro-images (Section 3.4.1).

## 3.5 Gravitational lensing in galaxy clusters

Giant luminous arcs (GLAs) in galaxy clusters represent the most spectacular effect of gravitational lensing (Figure 7t). They are produced by the merging of two or three lensed images of an extended background galaxy located close to the caustic (Figure 7). However, even after the discovery of the first multiply-imaged QSO in 1979, astronomers were not prepared to recognize the nature of those arcs.

It is worth quoting some comments made soon after the first observations of the arc in the galaxy cluster Abell 370 ($z = 0.373$; Figure 7t). Hoag (1981) reported in the *Bulletin of the American Astronomical Society*:

> Prime focus photographs taken with the Mayall 4-meter telescope at KPNO (Kitt Peak National Observatory) show a filament-like structure in the galaxy cluster Zw 0237.2−0146 (= Abell 370)... If the filament is associated with the cluster, its projected length, judged by the redshift and the diameters of the giant ellipticals, seems to be about 0.2 Mpc. Its width seems not to be resolved.

In 1986, the arc was independently re-observed (together with another one in the cluster Cl2242−02) by Lynds and Petrosian (1986), who wrote:

> We announce the existence of a hitherto unknown type of spatially coherent extragalactic structure having, in the most compelling known examples, the common properties: location in clusters of galaxies, narrow arc-like shape, enormous length, and situation of center of curvature towards both a cD galaxy and the apparent center of gravity of the cluster. The arcs are in excess of 100 kpc in length, have luminosity roughly comparable with those of giant E galaxies, and are distinctly bluer than E galaxies – especially in one case.

In 1987, Soucail and her collaborators reached similar quantitative conclusions, after introducing their observations in the following way (Soucail *et al.* 1987):

> The data reduction showed a strange ring-like condensation on the R-image very close to a bright elliptical

galaxy near the cluster center. The comparison of several images during the run proved that it was not an artifact.

Many tentative attempts to explain the arcs, in terms of, for example, cooling flows, bow shocks or light echoes, assumed that the arcs belonged to the cluster. Paczyński (1987) first realized that the shape, the orientation, the blue colour and the faint surface brightness of the arcs were a result of gravitational lensing. His prediction was confirmed by Soucail *et al.* (1988), who showed that the arc in Abell 370 was a strongly distorted view of a faint blue galaxy about twice as distant as the lensing cluster. Thus, after 51 years, Zwicky's prophecy was finally fulfilled!

Besides GLAs, galaxy clusters can also produce multiple images (Figure 11) or single distorted images (called arclets) of background galaxies.

In order to find more arcs, very deep ($B \sim 27$) and high-angular-resolution CCD frames of the richest galaxy clusters have been acquired. The best sample selects clusters with high X-ray luminosity rather than those with many galaxies as seen in the visible domain. For example, 8 arcs have been found by Luppino *et al.* (1999) among 38 clusters selected from the Einstein Observatory Extended Medium Sensitivity Survey (EMSS). Indeed, it is much more likely that an arc will be observed in a rich cluster than a multiply-imaged QSO will be found in a QSO sample because the population of faint blue galaxies discovered by Tyson (1988) yields a very dense grid of background sources. Furthermore, the angular scale of the arcs is 10 to 100 times larger than that of lensed QSO images.

Astronomers soon realized that gravitational arcs provide an excellent means of probing the central part of the galaxy clusters, including their dark matter content. Once the redshift of an arc is known, the central mass inside the Einstein radius can be approximated from eqn (6), with no assumption about

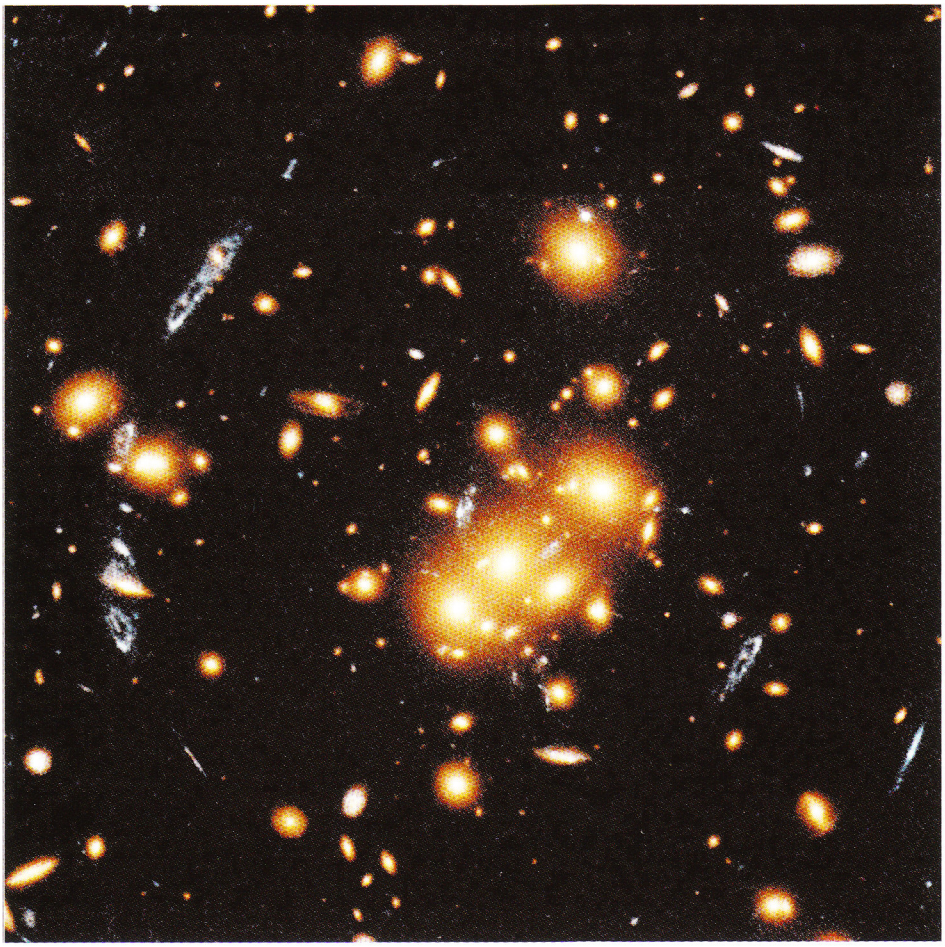

**Figure 11** Multiple images of a well-resolved blue background galaxy lensed by the galaxy cluster Cl0024 + 1654. This is a true-color image built from CCD frames obtained with the HST (Colley *et al.* 1996). (Courtesy of the Space Telescope Science Institute (STScI) operated for NASA by AURA and the Space Telescope European Coordinating Facility (ST-ECF).)

hydrostatic equilibrium of the gas. Typical masses and mass-to-light ratios derived from gravitational lensing are $M \sim 10^{14} M_{\odot}$ and $M/L_{\mathrm{B}} > 100$. They confirm that galaxy clusters are dominated by dark matter. The systematic discrepancy between the first values derived for cluster masses and those obtained from X-ray analyses seems to be progressively solved, partially by using more refined and specific lens models (Hattori *et al.* 2000). Once again, the HST's high angular resolution improved the lens models with new constraints coming from the detection of multiple images of galaxies (Figure 11) or new arcs. Very thin radial spokes have also been detected with the HST in the cluster Abell 370 (Figure 7t, although not visible in this rendition), MS0440 + 02 and AC118, indicating a central mass density distribution flatter than $r^{-2}$ and a small core radius.

As originally pointed out by Zwicky, lensing clusters may be used as natural telescopes to study faint background sources which would otherwise be out of reach. As mentioned in Section 2, a gravitational lens may help in two different ways: either it amplifies the total flux received from *unresolved* sources, or it improves the effective instrumental resolving power on *extended* objects by increasing their apparent size. The first property has been applied, for example, with the ISOCAM camera aboard the ISO satellite in order to detect mid-infrared sources intrinsically fainter than those directly observable outside the cluster. After correction for the lensing effects, we are left with a significant excess of sources with respect to the predictions, probably because of a higher star formation rate in those distant galaxies (Altieri *et al.* 1999). An interesting application of the second property has been made by Bunker *et al.* (2000), who used it in conjunction with the HST's high angular resolution to resolve the stellar populations in a lensed galaxy at $z = 4$; with the same technique, Franx *et al.* (1997) have discovered a lensed galaxy at $z = 4.92$ behind the cluster Cl1358 + 62.

The reader interested in gravitational lensing produced by galaxy clusters and its applications will find further details in the reviews by Fort and Mellier (1994) and Hattori *et al.* (2000).

## 3.6 Weak lensing

### 3.6.1 Weak lensing in galaxy clusters

Strong lensing – that is, multiple imaging with the possible formation of giant luminous arcs – is possible only when the misalignment between the source and the lens is typically smaller than the Einstein lens radius. The lens will still slightly distort the shape of background sources at much larger impact parameters: this is the so-called 'weak lensing' regime. The image of a circular source is an ellipse oriented along the local gravitational shear (perpendicular to the direction of the lens centre of mass), with an axis ratio equal to the ratio of the two eigenvalues of the magnification matrix (i.e. it is a function of the derivatives of the deflection angle). It is then easy to understand that, in principle, the mass distribution of the lens can be reconstructed from a dense grid of distorted background sources (Kaiser and Squires 1993, Bartelmann *et al.* 1996).

However, in practice the observations are difficult. First, a sufficiently dense grid of 40 galaxies per square arcminutes is reached for a limiting B magnitude of about 29 per square arc second (Tyson *et al.* 1990). Second, the induced ellipticity is only a few per cent, much smaller than the intrinsic ellipticity of galaxies, and a statistical analysis of a large number of (faint) background galaxies over a small area of the sky must be performed to retrieve the local orientation of the shear (atmospheric seeing and instrumental distortion also constitute sources of noise). Third, the redshift of the very faint background population is not known for sources located behind high-redshift lenses.

The first weak lensing effects were observed in the galaxy cluster Abell 370 by Fort *et al.* (1988), giving another confirmation of the lensed nature of GLAs (Figure 7t). Since then, weak lensing has been studied in more than twenty galaxy clusters, sometimes on scales larger than $1h^{-1}$ Mpc (as compared with $100\,h^{-1}$ kpc for strong lensing). The geometry of the recovered mass distribution is found to be in agreement with that derived from observations in visible light and X-rays, with mass-to-light ratios sometimes as large as $1000\,h^{-1}$ (median value of $300\,h^{-1}$; Mellier 1999).

### 3.6.2 Weak lensing in the Universe

The first angular correlation between bright quasars and foreground galaxies on a scale of 10 arc minutes was reported by Fugmann (1990). It has been interpreted by Bartelmann and Schneider (1993) as a consequence of the amplification bias (Section 2.6) due to the large-scale structures possibly associated with galaxies. Since then, other such angular correlations have been confirmed on the basis of independent observations. Moreover, weak shear has been detected around some selected bright quasars (Fort *et al.* 1996).

Very recently, correlated galaxy ellipticities have been detected by three independent teams in 'empty' large deep fields (where no foreground massive galaxy cluster was known). It is also a consequence of light deflection by the large-scale structures present in the Universe (Van Waerbeke *et al.* 2000, Wittman *et al.* 2000, Bacon *et al.* 2000).

We now reach the end of our trip in the world of lensing, by considering the whole Universe as a thick lens! The general situation is indeed much more complex than in the single-lens plane approximation described in Section 2, which is valid for strong lensing. Light bundles from very

distant galaxies and propagating across the Universe are sensitive not only to the expansion and geometry of spacetime, but also to the *total* quantity of matter present along their path. This is in contrast with traditional astronomical observations, which probe only the luminous content of the Universe – the visible 10% of the iceberg, as it were. The distortion of light bundles by the large-scale matter distribution present along the trajectory is called the *cosmic shear*. Its signature is the observed statistical correlation of the galaxy ellipticities, while its magnitude and angular scale depend on the mass of the dark matter distribution. It has been detected at a level smaller than 2.5% for angular scales typically less than 30 arcminutes.

The cosmic shear was first theoretically investigated by Blandford *et al.* (1991) and Miralda-Escudé (1991), in the context of the formation of large-scale structures. However, the observations are challenging because of the many systematic effects degrading the signal. More recent progress on the theoretical and observational sides makes it hopeful that this new technique can be applied to map the dark matter in the Universe at intermediate and low redshifts, and to measure the mass power spectrum without any assumption on the connection between dark and luminous matter. Ultimately this should help us in constraining the cosmological parameters, and to identify the intermediate stages between the very faint observed fluctuations of the cosmological microwave background and the presently observed structure of the Universe. Observations need to be extended to a lower shear level, corresponding to a larger angular scale.

Interested readers will find a more extended discussion of weak lensing in the Universe in the review by Mellier (1999).

## 4 FUTURE SPACE MISSIONS AND THEIR EXPECTED CONTRIBUTIONS TO THE FIELD

Taking advantage of the amplification bias in gravitational lens surveys (Section 2.6) and given the good (subarcsecond) angular resolution and high sensitivities of existing large optical telescopes and radio interferometers, we have seen in Section 3 that most of systematic observational searches for lenses had been carried out at optical, near-infrared and radio wavelengths. These brightest multiply-imaged quasars distributed all over the sky offer unique tools for decisive astrophysical and cosmological applications, including constraints on the cosmological parameters $\Omega_0$ and $\lambda_0$.

We naturally expect that during the first years of the new century, several large ground-based automated optical surveys will provide additional large samples of multiply-imaged quasars. These surveys include the Sloan Digital Sky Survey (SDSS; Castander 1998), the International Liquid Mirror Telescope (ILMT) project (Surdej and Claeskens 1997) and the Two Degree Field (2dF) survey (Boyle *et al.* 2000). Statistical and individual studies of such gravitational lens systems will enable us to address and/or to improve some of the astrophysical and cosmological applications discussed in Section 3.

### 4.1 GAIA – the galactic census

The GAIA mission has been selected as a future ESA cornerstone mission and scheduled for launch no later than 2012. It will then perform an on-target, multi-colour imaging and spectroscopic all-sky survey down to the limiting magnitude $V \sim 21$. The aimed astrometric accuracy of this survey is quite challenging: 10 micro-arcseconds at $V = 15$, and 200 milli-arcseconds at $V = 21$. Assuming that the GAIA onboard data analysis and selected data transmission to the ground will enable the identification of quasars showing a complex structure within a field of view of 3″, we have estimated that GAIA observations will lead to the detection of a complete sample of more than 3,500 gravitational lenses among optical quasars down to the limiting magnitude $V = 21$. This number has been derived for the less favorable Universe with $\Omega_0 = 1$, $\lambda_0 = 0$. In a universe with $\Omega_0 = 0$, $\lambda_0 = 1$, the total number of multiply-imaged quasars would be 13 times larger. All these results are, of course, independent of the Hubble constant $H_0$. If the field of view is further reduced to 2″ or 1″, only 83% or 46% of the gravitational lens systems will be detected, respectively. As expected, the contribution due to lensing galaxies of type E/S0 remains the most important one.

Furthermore, because of its unprecedented astrometric accuracy all over the sky, GAIA will follow the bending of star light by the Sun and the major planets over the entire celestial sphere and therefore directly observe the structure of spacetime. The accuracy of its measurements might lead to the detection of a discrepancy at the second order with the value predicted by GR. Measuring the $\gamma$ parameter (equal to unity in GR) of the parametrized post-Newtonian formulation of gravitational theories is of great importance to fundamental physics. So far, Hipparcos measurements have confirmed that $\gamma = 1.000 \pm 0.003$. GAIA measurements should improve the accuracy of the determination of $\gamma$ to the level of $5 \times 10^{-7}$, and thus might also test alternative cosmological theories, like the Brans–Dicke theory (Brans and Dicke 1961).

### 4.2 Submillimetre observations

In addition to the visible spectral range for bright quasars, and to a lesser extent the radio waveband, the amplification bias also turns out to be quite important in the submillimetre

waveband, for faint flux-limited samples of galaxies. Indeed, if the surface density of (unlensed) galaxies with an apparent magnitude brighter than $m$ is $n_U$ ($<m$), an amplification by a factor $\mu_T$ due to gravitational lensing will modify the counts as follows (Narayan 1989):

$$n_L(<m) = n_U(<m + 2.5\log(\mu_T))/\mu_T \quad (18)$$

The factor $n_U$ ($<m + 2.5\log(\mu_T)$) accounts for the increase in the observed number of galaxies due to the fact that objects as faint as $m + 2.5\log(\mu_T)$ can now become brighter than the limiting magnitude $m$, as a result of gravitational lensing amplification by a factor of $\mu_T$. However, the galaxies we observe projected in the lens (sky) plane within a solid angle $d\omega$ are actually located within a smaller solid angle $d\omega_s$ ($=d\omega/\mu_T$) in the source plane, so that their observed surface density must be decreased by a factor of $d\omega/d\omega_s$ (eqns (4) and (9)), accounting for the factor $1/\mu_T$ in eqn (18). If $s$ represents the slope of the logarithmic intrinsic number counts of objects as a function of apparent magnitude $m$, such that

$$s = \frac{d}{dm}(\log(n_U(<m))), \quad (19)$$

eqn. (18) may then be rewritten as

$$n_L(<m) = n_U(<m)\mu_T^{2.5s-1} \quad (20)$$

Depending on the value of the slope $s$ ($\geq 0.4$ or $<0.4$), we see that the surface density of galaxies $n_L(<m)$ will either be larger or smaller than the original number and the amplification bias $\mu_T^{2.5s-1}$ will either be larger or smaller than 1. The amplification bias was first discussed in the context of bright QSO surveys at optical wavelengths; however, Blain (1997) has pointed out that the number counts of faint galaxies in the submillimetre waveband are extremely steep, with observed values of $s$ even larger than 1.2 (Blain and Longair 1993, 1996). We thus expect the amplification bias induced by galaxy lensing or galaxy cluster lensing in the submillimetre domain to be very high for faint galaxies, and that the largest excess of lenses will occur at flux densities where the submillimetre counts are the steepest. (From Figure 2 in Blain (1997), we find that, typically, the flux is 0.1, 0.2, 0.5, 0.2 and 0.1 Jy at wavelenghts of 1300, 850, 450, 200 and 90 μm, respectively.) Note that the slope $s$ of the counts decreases from longer to shorter wavelengths; the 90 μm counts becoming similar to those at optical wavelengths. Adopting $H_0 = 50\,\mathrm{km\,s^{-1}\,Mpc^{-1}}$, and various values for the cosmological parameters $\Omega_0$ and $\lambda_0$, Blain (1997, 1998a,b) gives estimates for the number counts of faint distant dusty star-forming galaxies and AGNs (active galactic nuclei) at different wavelengths in the submillimetre waveband, under different assumptions (evolving and non-evolving mass distributions of lensing galaxies, different world models, different types of evolution of the source galaxies). As expected, the main conclusion is that the ratio of lensed to unlensed integral counts of faint galaxies in the submillimetre region is highest at $\lambda = 1300$ μm (approximately 3%), then gradually decreases with wavelength (to 1.7% at $\lambda = 850$ μm, 0.8% at $\lambda$ 450 μm, 0.3% at $\lambda = 200$ μm and only 0.04% at $\lambda = 90$ μm). (For comparison, the ratio of lensed to unlensed HLQs in optical samples is of the order of 1% (Surdej *et al.* 1993), and approximately 0.1% for radio sources.) Note, however, that above $\lambda = 200$ μm the surface density of both lensed and unlensed galaxies decreases as the wavelength of observation increases, and that a best compromise ought to be sought between a high ratio of lensed to unlensed galaxies and a high total number of lensed galaxies.

### 4.3 The Herschel Space Observatory and the Planck mission

A clever combination of wide-field surveys obtained by space instruments, such as the forthcoming Herschel Space Observatory (originally named the Far Infrared and Submillimetre Space Telescope (FIRST) satellite) and Planck Surveyor, with the high flux sensitivity and angular resolution of large ground-based submillimetre/millimetre interferometer arrays (such as ALMA, the Atacama Large Millimetre Array), ought to provide a large sample of gravitational lens systems. Several hundred lenses should be identified, and these will be ideally suited to probe the distant Universe as well as to infer the properties, evolution and so on of the faintest and most distant populations of galaxies in the Universe.

From simulations made by Blain (1997, 1998a,b) at wavelengths of 200, 450 and 850 μm, an all-sky survey carried out by Planck should contain approximately 650, 560 and 40 gravitational lenses out of a total population of 240,000, 71,000 and 2,300 unlensed galaxies, respectively. However, the 4′ angular resolution of Planck is not good enough to allow rapid and efficient follow-up observations of those galaxies from the ground. But at $\lambda = 850$ μm, HSO could be used to determine more accurate (subarcminute) positions and flux densities of the 2300 galaxies in a relatively short time. These candidates could then be observed in a snapshot mode and/or be further studied with large ground-based submillimetre/millimetre interferometer arrays. However, it is not yet clear how best to select the candidates at shorter wavelengths. As suggested by Blain (1997, 1998a,b), it is likely that 'colour' information provided by the HSO and/or Planck observatories will enable the gravitational lens candidates to be extracted from all the faint submillimetre sources that will be detected. Indeed, because most of the lensed galaxies will be found at large

redshifts, one would expect that if the dust temperature in star-forming galaxies is correlated with their luminosity, lensed galaxies will systematically show redder colours than will unlensed galaxies observed at the same flux densities.

Note that optimal targets to search for amplified (Herschel/Planck) and/or magnified (ALMA) submillimetre galaxies are foreground galaxy clusters. The lensed images of faint galaxies are expected to be the brightest sources of submillimetre wave radiation on arc second scales. Although these lensed galaxies could not be resolved by Herschel, they will increase the level of source confusion noise in the direction of the galaxy cluster as compared with observations in the field (Blain 1997, 1998a,b). These could subsequently be observed with large ground-based submillimetre/millimetre interferometric arrays. Herschel observations of catalogued galaxy clusters and many more clusters to be found with the Newton X-ray satellite (orginally known as the X-ray Multimirror Mission, XMM) as well as with Planck could also be used to investigate the gravitational lensing effects of clusters on the population of faint background galaxies emitting large amounts of energy in the submillimetre waveband.

NGST, with its imaging spectroscopy device and direct imaging capabilities in the near- and mid-infrared, will be an ideal telescope to further study and extend the spectral range of studies of gravitational lens candidates that will by then have been identified in the (sub-)millimetre domain. Similarly, the Advanced Camera and/or the WFPC3 camera that will be available aboard HST in the near future should also provide a unique mapping at ultraviolet and optical wavelengths of weak lensing around the galaxy clusters targeted with the Herschel and Planck.

### 4.4 The MAP mission

From 2001, the Microwave Anisotropy Probe (MAP) satellite will provide a detailed mapping of the microwave background radiation, with a much higher sensitivity than COBE (Cosmic Background Explorer) and an angular resolution approximately 35 times better. (The international Boomerang balloon experiment has provided interesting clues on the detailed structure of the microwave cosmic background over a small sky area that suggest that our Universe is flat (de Bernardis *et al.* 2000).) Planck's observations should be of still much higher quality, but will not start before 2007. Analysis of the MAP data should not only lead to a very precise determination of the cosmological parameters ($H_0$, $\Omega_0$ and $\lambda_0$) and of the fraction of visible versus dark matter, but also test whether our view of an infinite Universe filled with all its known and unknown constituents could not actually result from a cosmic illusion on the scale of the Universe itself. Could it be that a large fraction of the billions of visible galaxies and quasars are only the repeated images of a much smaller number of galaxies in a finite Universe? Could most of these images just be the result of light emitted from a much smaller number of galaxies, circling the whole finite Universe along different trajectories and seen at different epochs of their cosmic evolution, possibly including images of our own Milky Way? The MAP data will be used by theorists to search for repeated or redundant temperature patterns over the cosmic microwave background which could arise in a finite Universe (Roukema and Luminet 1999). In addition, the specific age of any observed cosmic mirage would depend on the precise size and overall shape of the Universe. Theorists are eagerly awaiting the MAP observations to test this alternative theory.

### 4.5 X-ray observations

Owing to the low surface density of X-ray sources in the sky and their simple source structure, gravitational lens systems ought to be easily identified from the multiplicity of their X-ray images, provided the angular resolution of the X-ray telescope is good enough. Muñoz *et al.* (1999b) estimated the expected number of multiply-imaged AGNs in the soft X-ray band (0.3–3.5 kev) as a function of the flux limit. They find that approximately 1, 0.1 and 0.01 multiple X-ray images of AGNs lensed by foreground galaxies should be found per square degree down to fluxes of $10^{-15}$, $10^{-14}$ and $10^{-13}$ erg $s^{-1}$ $cm^{-2}$, respectively. Muñoz *et al.* (1999b) found the maximum value for the ratio of lensed to unlensed X-ray sources to be about 0.2–0.4% in the flux range $10^{-13}$–$10^{-12}$ erg $s^{-1}$ $cm^{-2}$. Taking into account the observational selection function of the HRC (High Resolution Camera) and ACIS (AXAF CCD Imaging Spectrometer) detectors aboard the Chandra X-ray Observatory (CXO, originally known as the Advanced X-ray Astrophysics Facility, AXAF), they found that about 1–3 such lensed sources should be detected serendipitously per year of high-resolution imaging. Such an estimate is almost independent of the flux limit. This low detection rate is essentially due to the small field of view of Chandra. The same authors also determined that if Chandra were used to take deep images of known rich galaxy clusters at intermediate redshifts, one wide-separation, multiply-imaged background X-ray source should be detected down to the above flux limits for every 10, 30 and 300 clusters. Of course, such a programme would occupy a substantial amount of observing time (at least several months).

Because of the wider field of view and high sensitivity of the European XMM-Newton telescope, the prospects for detecting gravitationally lensed images look rather more promising. XMM-Newton's angular resolution is coarser (5″ FWHM) than that of Chandra, but the identification of the multiply-imaged AGNs would rely on a parallel high-angular-resolution optical survey, as planned by the XMM–LSS (Large Scale Structures) Consortium. In this

framework, we estimate that the planned XMM–LSS imaging of 64 square degrees with typical exposure times of about 3 hours should lead to the detection of some 20 X-ray sources lensed by foreground galaxies. XMM-Newton would also turn out to be very useful for the detection of lensed objects by intervening clusters. Typically, the XMM–LSS survey should identify approximately 700 galaxy clusters for which some 40 multiply-imaged background X-ray sources ought to be found.

Given the unique high-angular-resolution capabilities of Chandra, this observatory will very likely be used to investigate the photometric and spectroscopic properties of known lensed quasars and/or their individual lensed images with X-ray luminosities that are a factor of $\mu$ (their gravitational lens amplification) smaller than unlensed quasars at a comparable flux limit, and to estimate the contribution of such faint quasars to the X-ray cosmic background. Chandra will also certainly play a part in monitoring the fast X-ray variability of known multiply-imaged QSOs with a high time resolution, allowing one to derive much more accurate time delays between the multiple lensed images. Shorter microlensing events could also be probed.

An X-ray observatory with an angular resolution comparable to, or better than that of Chandra and a field of view similar to, or larger than, that of XMM-Newton would be the ideal instrument with which to search the whole sky for a large number of multiple X-ray source images lensed by foreground galaxies and clusters. Lenses would then be directly recognizable as such on the sole basis of the X-ray data.

## 5 SUMMARY AND CONCLUSIONS

Gravitational lensing creates an intimate relation between the observer, a massive astrophysical object (the gravitational lens), a luminous source and the whole Universe (eqn (3)). We conclude by considering what we have learnt or still hope to learn about each of these four components.

Observers are human beings. The historical part of this chapter has retold an interesting journey into the human mind and psychology, and ultimately into the way of making science. A genius (Einstein!) finds the theoretical location of a gold mine. However, he is very rich and does not feel the need to exploit this mine or even to explore it further. He leaves that to the community. But the mine is located in a wild, unexplored region of human knowledge. Few people want to go there, but even the most adventurous of them are unable to reach the mine. Only theoreticians can dream of it. Most scientists are realistic people who do not believe in gold mines. Many years after the genius's revelation, someone accidentally discovers the mine, as mysterious as a temple in the jungle, but cannot keep its location secret. Soon, pioneers arrive and prepare an easy access to the site, and then many scientists rush to the mine, eager to explore every logical passage. This is the start of the golden age.

Today, the deflection of light by massive bodies, as predicted by Einstein's theory of general relativity, has been measured in the Solar System, in the Milky Way and on extragalactic scales. Thanks to this theory, a large variety of observed effects – image shifts, multiple images, giant arcs, radio rings, time delays, flux variations or weak shear distortions of background sources – can all be qualitatively explained by the gravitational influence of normal stars, galaxies, galaxy clusters or large-scale structures. The deflection angle ranges from micro-arcseconds to tens of arcseconds. It has also been checked to be wavelength independent from the far UV to the radio domain. Since the deflection angle is very small, the basic formalism of gravitational lensing is rather simple, as shown in Section 2.

Gravitational lensing does not only prove general relativity to be a correct description of reality, but it also provides a powerful tool to investigate astrophysical objects and the Universe (Section 3).

Let us now turn to the lenses themselves. Since gravity acts also on light, studying the luminous shapes of background sources yields information on the nature of the foreground lens population. In particular, gravitational lensing has confirmed the presence of large amounts of dark matter in the Universe, associated with external galaxies, galaxy clusters and large-scale structures. The mass-to-light ratio in some clusters can indeed be as high as 1000. However, gravitational lensing shows that if isolated, cosmologically distributed compact dark objects exist, their spatial density is probably not high enough to close the Universe. However, it is not yet clear whether the microlensing events detected in the direction of the LMC are due to dark compact objects located in the halo of the Milky Way.

The multiple image configurations produced by individual lensing galaxies are compatible with those produced by isothermal and singular matter distributions. Gravitational lensing will also enable us in the near future to probe quantitatively the extinction law of those distant galaxies. Galactic microlensing is promising for the detection of planets orbiting the main stellar lens.

Our knowledge of the sources may be improved with gravitational lensing by taking advantage of the so-called 'telescope effect', predicted by Zwicky as early as 1937. Striking examples are the discovery of a very distant galaxy at $z = 4.92$ located behind the galaxy cluster Cl1358 + 62 and the study of stellar populations in a $z = 4$ galaxy. Massive galaxy clusters have also helped in detecting a more distant population of dusty galaxies at submillimetre wavelengths (Smail *et al.* 1997). The continuum size of quasars has been constrained from microlensing observations, and theoretical studies indicate that extragalactic microlensing

could even help in resolving the structure of quasar accretion disks (Agol and Krolik 1999). Microlensing in our Galaxy should allow us to study the surface of stars; the limb darkening of a lensed star has indeed already been measured (Sackett 2001, and references therein).

The global properties of the Universe, in which light is travelling from the source to the observer, leave their imprint on the multiply-lensed images of extragalactic sources. The Hubble constant has been derived for several cases from time-delay measurements between flux variations of multiply-imaged QSOs, and the value of the cosmological constant has been constrained from the number of multiply-imaged quasars in optical and radio QSO samples. Gravitational lensing represents an alternative approach to the classical methods and avoids the traditional issue of intermediate standard flux calibrations. However, this technique has its own drawbacks: the determination of $H_0$ is limited by the poor knowledge of the lens model, and the derived value of $\lambda_0$ is sensitive to the incompleteness of the parent QSO sample (selection biases, dust extinction and so on) as well as to the luminosity function of the source population, which is not very well known (especially for radio sources). Homogeneous QSO samples coming from automated surveys (e.g. SDSS, 2dF, ILMT), optical identifications of radio sources analysed by CLASS, and new observations of (new) lenses adequate to constrain the lens model may improve the situation in the near future. We may also believe in our Lucky Star, since Link and Pierce (1998) showed that if we had the chance to observe multiple arcs from sources located behind a given cluster but at different redshifts, the cosmological model could then be determined with a better precision.

We cannot conclude this chapter without coming back to the observers. Observations of gravitational lenses are very demanding in terms of spatial resolution and collecting power, but also in time sampling for flux monitoring or in data handling for microlensing searches in the Milky Way. These difficulties have motivated much work in image processing (e.g. point spread function (PSF) subtraction or deconvolution), in light-curve analysis and in team organization to carry out sustained photometric monitoring campaigns in order to obtain frequent data. In this context, space observations, especially with the HST, have played a crucial role with respect to the angular resolution issue. Most gravitational lenses have been discovered with ground-based telescopes or radio telescopes, but the HST has enlightened us with the confirmation of several cases with small angular separations (like J03.13, Figure 9), with the precise determination of all the lensed image positions, with discoveries of new arcs and the first detection of several lensing galaxies.

Where are we going now? Strong lensing events such as giant arcs or multiply-imaged sources are rare, but automated surveys with (nearly) full-sky coverage (SDSS, CLASS, ILMT, GAIA) will find them more and more systematically. Weak shear distortions are common but difficult to detect; however, the increasing accuracy of both observations and analysis has yielded encouraging results very recently (Section 3.6). Gravitational lenses are no longer rare scientific jewels. Until now, either we have usually assumed a known background source population in order to study the lensing population, or we have estimated the distortion of the apparent properties of a class of sources, assuming a given foreground lens population. In reality, both problems are intrinsically connected and should be solved simultaneously. It will probably be impossible to do so, but there is no doubt that in the future, gravitational lensing will help to build a coherent three-dimensional image of the Universe. We are thus now entering the Iron Age of gravitational lensing!

### Acknowledgments

Our research was supported in part by contract P4/05 'Pôle d'Attraction Interuniversitaire' (OSTC, Belgium), by PRODEX (Gravitational lens studies with HST) and by the 'Fonds National de la Recherche Scientifique' (Belgium). We are very grateful to Jean-Pierre Swings for reading the manuscript and to Anna Pospieszalska for her help with some of the figures, the table and the bibliography.

## FURTHER READING

Further reading on gravitational lensing includes the textbook by Schneider, Ehlers and Falco (1992), the book in Russian by Bliokh and Minakov (1989) and review papers by Blandford and Narayan (1992), Refsdal and Surdej (1994), Fort and Mellier (1994), Narayan and Bartelmann (1996), Wambsganss (1998), Mellier (1999) and Claeskens and Surdej (2001). We refer the reader to the book by Peterson (1997) for a general introduction to active galactic nuclei and quasars.

## REFERENCES

Agol, E. and Krolik, J. (1999). Imaging a quasar accretion disk with microlensing. *Astrophysical Journal*, **524**, 49–64.

Albrow, M., Beaulieu, J-P., Birch, P., Caldwell, J.A.R., Kane, S., Martin, R., Menzies, J., Naber, R.M., Pel, J.-W., Pollard, K., Sackett, P.D., Sahu, K.C., Vreeswijk, P., Williams, A. and Zwaan, M.A. (1998). The 1995 pilot campaign of PLANET: Searching for microlensing anomalies through precise, rapid, round-the-clock monitoring. *Astrophysical Journal*, **509**, 687–702.

Alcock, C., Allsman, R.A., Alves, D.R., Axelrod, T.S., Becker, A.C., Bennett, D.P., Cook, K.H., Dalal, N., Drake, A.J., Freeman, K.C., Geha, M.,

Griest, K., Lehner, M.J., Marshall, S.L., Minniti, D., Nelson, C.A., Peterson, B.A., Popowski, P., Pratt, M.R., Quinn, P.J., Stubbs, C.W., Sutherland, W., Tomaney, A.B., Vandehei, T. and Welch, D. (2000). The MACHO Project: Microlensing results from 5.7 years of LMC observations. *Astrophysical Journal*, **542**, 281–307.

Altieri, B., Metcalfe, L., Kneib, J-P., McBreen, B., Aussel, A., Biviano, A., Delaney, M., Elbaz, D., Leech, K., Lémonon, L., Okumura, K., Pelló, R. and Schulz, B. (1999). An ultra-deep ISOCAM observation through a cluster-lens. *Astronomy and Astrophysics*, **343**, L65–L69.

Angonin-Willaime, M-C., Vanderriest, C., Courbin, F., Burud, I., Magain, P. and Rigaud, F. (1999). About the origin of extinction in the gravitational lens system MG J0414 + 0534. *Astronomy and Astrophysics*, **347**, 434–441.

Aubourg, E. and Palanque-Delabrouille, N. (1999). A search for galactic dark matter with EROS 2. *New Astronomy*, **4**, 265–273.

Bacon, D., Refregier, A. and Ellis, R. (2000). Detection of weak gravitational lensing by large-scale structure. *Monthly Notices of the Royal Astronomical Society*, **318**, 625–640.

Barnothy, J.M. (1965). Quasars and the gravitational image intensifier. *Astronomical Journal*, **70**, 666.

Bartelmann, M., Narayan, R., Seitz, S. and Schneider, P. (1996). Maximum-likelihood cluster reconstruction. *Astrophysical Journal*, **464**, L115–L118.

Bartelmann, M. and Schneider, P. (1993). Large-scale QSO-galaxy correlations revisited. *Astronomy and Astrophysics*, **271**, 421–424.

de Bernardis, P., Ade, P.A.R., Bock, J.J., Bond, J.R., Borrill, J., Boscaleri, A., Coble, K., Crill, B.P., De Gasperis, G., Farese, P.C., Ferreira, P.G., Ganga, K., Giacometti, M., Hivon, E., Hristov, V.V., Iacoangeli, A., Jaffe, A.H., Lange, A.E., Martinis, L., Masi, S., Mason, P.V., Mauskopf, P.D., Melchiorri, A., Miglio, L., Montroy, T., Netterfield, C.B., Pascale, E., Piacentini, F., Pogosyan, D., Prunet, S., Rao, S., Romeo, G., Ruhl, J.E., Scaramuzzi, F., Sforna, D. and Vittorio, N. (2000). A flat Universe from high-resolution maps of the cosmic microwave background radiation. *Nature*, **404**, 955–959.

Bernstein, G. and Fischer, P. (1999). Values of $H_0$ from models of the gravitational lens 0957 + 561. *Astronomical Journal*, **118**, 14–34.

Blain, A.W. (1997). Gravitational lensing by clusters of galaxies in the millimetre/submillimetre waveband. *Monthly Notices of the Royal Astronomical Society*, **290**, 553–565.

Blain, A.W. (1998a). The Planck Surveyor mission and gravitational lenses. *Monthly Notices of the Royal Astronomical Society*, **297**, 511–516.

Blain, A W. (1998b). Submillimetre-wave gravitational lenses and cosmology. *Monthly Notices of the Royal Astronomical Society*, **295**, 92–98.

Blain, A.W. and Longair, M.S. (1993). Submillimetre cosmology. *Monthly Notices of the Royal Astronomical Society*, **264**, 509–521.

Blain, A.W. and Longair, M.S. (1996). Observing strategies for blank-field surveys in the submillimetre waveband. *Monthly Notices of the Royal Astronomical Society*, **279**, 847–858.

Blandford, R.D. and Narayan, R. (1992). Cosmological applications of gravitational lensing. *Annual Review of Astronomy and Astrophysics*, **30**, 311–358.

Blandford, R.D., Saust, A.B., Brainerd, T.G. and Villumsen, J.V. (1991). The distortion of distant galaxy images by large scale structure. *Monthly Notices of the Royal Astronomical Society*, **251**, 600–627.

Bliokh, P.V. and Minakov, A.A. (1989). *Gravitatsionnye Linzy* [Gravitational Lensing], Naukova Dumka, Kiev.

Borgeest, U. (1986). Determination of galaxy masses by the gravitational lens effect. *Astrophysical Journal*, **309**, 467–471.

Bourassa, R.R. and Kantowski, R. (1975). The theory of transparent gravitational lenses. *Astrophysical Journal*, **195**, 13–21.

Bourassa, R.R., Kantowski, R. and Norton, T.D. (1973). The spheroidal gravitational lens. *Astrophysical Journal*, **185**, 747–756.

Boyle, B.J., Shanks, T., Croom, S.M., Smith, R.J., Miller, L., Loaring, N. and Heymans, C. (2000). The 2dF QSO Redshift Survey – I. The optical QSO luminosity function. *Monthly Notices of the Royal Astronomical Society*, **317**, 1014–1022.

Boyle, B.J., Shanks, T., Peterson, B.A. (1988). The evolution of optically selected QSOs. II. *Monthly Notices of the Royal Astronomical Society*, **235**, 935–948.

Brans, C. and Dicke, R.H. (1961). Mach's principle and a relativistic theory of gravitation. *Physical Review*, **124**, 925–935.

Bunker, A.J., Moustakas, L.A. and Davis, M. (2000). Resolving the stellar populations in a $z = 4$ lensed galaxy. *Astrophysical Journal*, **531**, 95–117.

Burke, W.L. (1981). Multiple gravitational imaging by distributed masses. *Astrophysical Journal*, **244**, L1.

Burud, I., Courbin, F., Lidman, C., Jaunsen, A., Hjorth, J., Ostensen, R., Andersen, M.I., Clasen, J.W., Wucknitz, O., Meylan, G., Magain, P., Stabell, R. and Refsdal, S. (1998). High-resolution optical and near-infrared imaging of the quadruple quasar RX J0911.4 + 0551. *Astrophysical Journal*, **501**, L5–L10.

Canizares, C.R. (1982). Manifestations of a cosmological density of compact objects in quasar light. *Astrophysical Journal*, **263**, 508–517.

Castander, F.J. (1998). The Sloan Digital Sky Survey. *Astrophysics and Space Science*, **263**, 91–94.

Chae, K-Y. (1999). New modeling of the lensing galaxy and cluster of Q0957 + 561: Implications for the global value of the Hubble constant. *Astrophysical Journal*, **524**, 582–590.

Chwolson, O. (1924). Über eine mögliche Form fiktiver Doppelsterne. *Astronomische Nachrichten*, **221**, 329.

Claeskens, J-F. (1999). Thèse de Doctorat. Aspects statistiques du phénomène de lentille gravitationnelle dans un échantillon de quasars très lumineux. *Societé Royale des Sciences de Liège*, **68**, 1–305.

Claeskens, J-F. and Surdej, J. (2001). Gravitational lensing in quasar samples. *Astronomy and Astrophysics Review*, in the press.

Claeskens, J-F., Surdej, J. and Remy, M. (1996). J03.13A and B: A new multiply imaged QSO candidate. *Astronomy and Astrophysics*, **305**, L9–L12.

Colley, W.N., Tyson, J.A. and Turner, E.L. (1996). Unlensing multiple arcs in 0024 + 1654: Reconstruction of the source image. *Astrophysical Journal*, **461**, L83–L86.

Cooray, A.R. (1999). Cosmological parameters from statistics of strongly lensed radio sources. *Astronomy and Astrophysics*, **342**, 353–362.

Dalcanton, J.J., Canizares, C.R., Granados, A., Steidel, C.C. and Stocke, J.T. (1994). Observational limits on Omega in stars, brown dwarfs, and stellar remnants from gravitational microlensing. *Astrophysical Journal*, **424**, 550–568.

D'Odorico, V., Cristiani, S., D'Odorico, S., Fontana, A., Giallongo, E. and Shaver, P. (1998). The size and geometry of the Ly$\alpha$ clouds. *Astronomy and Astrophysics*, **339**, 678–686.

Dyer, C.C. and Roeder, R.C. (1972). The distance–redshift relation for universes with no intergalactic medium. *Astrophysical Journal*, **174**, L115–L117.

Dyson, F.W., Eddington, A.S. and Davidson, C.R. (1920). A determination of the deflection of light by the sun's gravitational field, from observations made at the total eclipse of May 29, 1919. *Memoirs of the Royal Astronomical Society*, **62**, 291–333.

Eddington, A.S. (1920). *Space, Time and Gravitation*. Cambridge University Press.

Einstein, A. (1936). Lens-like action of a star by the deviation of light in the gravitational field. *Science*, **84**, 506–507.

Etherington, I.M.H. (1933). On the definition of distance in general relativity. *Philosophical Magazine*, **15**, 761.

Falco, E.E., Gorenstein, M.V. and Shapiro, I.I. (1985). On model dependent bounds on $H_0$ from gravitational images: Application to Q0957 + 561 A, B. *Astrophysical Journal*, **289**, L1–L4.

Falco, E.E., Kochanek, C.S. and Muñoz, J.A. (1998). Limits on cosmological models from radio-selected gravitational lenses. *Astrophysical Journal*, **494**, 47–59.

Fomalont, E.B. and Sramek, R.A. (1975a). A confirmation of Einstein's general theory of relativity by measuring the bending of microwave radiation in the gravitational field of the Sun. *Astrophysical Journal*, **199**, 749–755.

Fomalont, E.B. and Sramek, R.A. (1975b). Measurements of the solar gravitational deflection of radio waves in agreement with general relativity. *Physical Review Letters*, **36**, 1475–1478.

Fort, B. and Mellier, Y. (1994). Arc(let)s in clusters of galaxies. *Astronomy and Astrophysics Review*, **5**, 239–292.

Fort, B., Mellier, Y., Dantel-Fort, M., Bonnet, H. and Kneib, J-P. (1996). Observations of weak lensing in the fields of luminous radiosources. *Astronomy and Astrophysics*, **310**, 705–714.

Fort, B., Prieur, J.L., Mathez, G., Mellier, Y. and Soucail, G. (1988). Faint distorted structures in the core of A 370: Are they gravitationally lensed galaxies at $z = 1$? *Astronomy and Astrophysics*, **200**, L17–L20.

Franx, M., Illingworth, G.D., Kelson, D., van Dokkum, P.G. and Tran, K-V. (1997). A pair of lensed galaxies at $z = 4.92$ in the field of Cl1358 + 62. *Astrophysical Journal*, **486**, L75–L78.

Froeschlé, M., Mignard, F. and Arenou, F. (1997). Determination of the PPN parameter $\gamma$ with the Hipparcos data. In *Proceedings of the ESA Symposium 'Hipparcos Venice'97'*, ESA SP-402, pp. 49–52.

Fugmann, W. (1990). Statistical gravitational lensing and the Lick Catalogue of galaxies. *Astronomy and Astrophysics*, **240**, 11–21.

Fukugita, M., Futamase, T. and Kasai, M. (1990). A possible test for the cosmological constant with gravitational lenses. *Monthly Notices of the Royal Astronomical Society*, **246**, 24P–27P.

Gebhardt, K., Richstone, D., Ajhar, E.A., Lauer, T.R., Byun, Y-I., Kormendy, J., Dressler, A., Faber, S.M., Grillmair, C. and Tremaine, S. (1996). The centers of early-type galaxies with HST: III. Non-parametric recovery of stellar luminosity distribution. *Astronomical Journal*, **112**, 105–113.

Gondhalekar, P.M. and Wilson, R. (1980). UV spectra of the twin QSOs 0957 + 561 A, B. *Nature*, **285**, 461–463.

Gorenstein, M.V., Falco, E.E., Shapiro, I.I., (1988). Degeneracies in parameter estimates for models of gravitational lens systems. *Astrophysical Journal*, **327**, 693–711.

Gott, J.R. III (1981). Are heavy halos made of low mass stars? A gravitational lens test. *Astrophysical Journal*, **243**, 140–146.

Hartwick, F.D.A. and Schade, D. (1990). The space distribution of quasars. *Annual Review of Astronomy and Astrophysics*, **28**, 437–489.

Hattori, M., Kneib, J-P. and Makino, N. (1999). Gravitational lensing in clusters of galaxies. *Progress of Theoretical Physics*, Suppl., **133**, 1.

Helbig, P., Marlow, D.R., Quast, R., Wilkinson, P.N., Browne, W.A. and Koopmans, L.V.E. (1999). Gravitational lensing statistics with extragalactic surveys: II. Analysis of the Jodrell Bank-VLA Astrometric Survey. *Astronomy and Astrophysics Supplement*, **136**, 297–305.

Hoag, A. (1981). A feature in the galaxy cluster Zw0237.2-0146. *Bulletin of the American Astronomical Society*, **13**, 799.

Jean, C. and Surdej, J. (1998). Redshift estimation of a gravitational lens from the observed reddening of a multiply imaged quasar. *Astronomy and Astrophysics*, **339**, 729–736.

Kaiser, N. and Squires, G. (1993). Mapping the dark matter with weak gravitational lensing. *Astrophysical Journal*, **404**, 441–450.

Kassiola, A., Kovner, I. and Blandford, R.D. (1991). Bounds on intergalatic compact objects from observations of compact radio sources. *Astrophysical Journal*, **381**, 6–13.

Kayser, R., Helbig, P. and Schramm, T. (1997). A general and practical method for calculating cosmological distance. *Astronomy and Astrophysics*, **318**, 680–686.

Kochanek, C.S. (1996). Is there a cosmological constant? *Astrophysical Journal*, **466**, 638–659.

Klimov, Y.G. (1963). The deflection of light rays in the gravitational fields of galaxies. *Soviet Physics Doklady*, **8**, 119–122.

Kundić, T., Turner, E.L., Colley, W.N., Gott, R. III, Rhoads, J.E., Wang, Y., Bergeron, L.E., Gloria, K.A., Long, D.C., Malhotra, S. and Wambsganss, J. (1997). A robust determination of the time delay in 0957 + 561A,B and a measurement of the global value of Hubble's constant. *Astrophysical Journal*, **482**, 75–82.

Lebach, D.E., Corey, B.E., Shapiro, I.I., Ratner, M.I., Webber, J.C., Rogers, A.E.E., Davis, J.L. and Herring, T.A. (1995). Measurement of the solar gravitational deflection of radio waves using very-long-baseline interferometry. *Physical Review D*, **75**, 1439–1442.

Liebes, S. (1964). Gravitational lenses. *Physical Review B*, **133**, 835–844.

Link, R. and Pierce, M.J. (1998). Cosmological parameters from multiple-arc gravitational lensing systems: I. Smooth lensing potentials. *Astrophysical Journal*, **502**, 63–74.

Lodge, O.J. (1919). Gravitation and light. *Nature*, **104**, 354.

Luppino, G.A., Gioia, I.M., Hammer, F., Le Fèvre, O. and Annis, J.A. (1999). A search for gravitational lensing in 38 X-ray selected clusters of galaxies. *Astronomy and Astrophysics*, Suppl., **136**, 117–137.

Lynds, R. and Petrosian, V. (1986). Giant luminous arcs in galaxy clusters. *Bulletin of the American Astronomical Society*, **18**, 1014.

Maoz, D. and Rix, H-W. (1993). Early-type galaxies, dark halos, and gravitational lensing statistics. *Astrophysical Journal*, **416**, 425–443.

Marani, G.F., Nemiroff, R.J., Norris, J-P., Hurley, K. and Bonnell, J.T. (1999). Gravitationally lensed gamma-ray bursts as probes of dark compact objects. *Astrophysical Journal*, **512**, L13–L16.

Mellier, Y. (1999). Probing the Universe with weak lensing. *Annual Review of Astronomy and Astrophysics*, **37**, 127–189.

Miralda-Escudé, J. (1991). The correlation function of galaxy ellipticities produced by gravitational lensing. *Astrophysical Journal*, **380**, 1–8.

Muñoz, J.A., Falco, E.E., Kochanek, C.S., Lehár, J., McLeod, B.A. Impey, C.D., Rix, H.-W., Peng, C.Y. (1999a). The CASTLES project. In: J. Gorgas and J. Zamorano (eds), *Astrophysics and Space Science*, (special issue: Proc. III Scientific Meeting of the SEA), astro-ph/9902131.

Muñoz, J.A., Kochanek, C.S. and Falco, E.E. (1999b). Finding gravitational lenses with X-rays. *Astrophysical Journal*, **521**, L17–L20.

Nadeau, D., Yee, H.K.C., Forrest, W.J., Garnett, J.D., Ninkov, Z. and Pipher, J.L. (1991). Infrared and visible photometry of the gravitational lens system 2237 + 030. *Astrophysical Journal*, **376**, 430–438.

Narayan, R. and Bartelmann, M. (1996). Lectures on gravitational lensing. In A. Dekel and J.P. Ostriker (eds), *Formation of Structure in the Universe*, Proceedings of the 1995 Jerusalem Winter School, Cambridge University Press.

Narayan, R. (1989). Gravitational lensing and quasar–galaxy correlations. *Astrophysical Journal*, **339**, L53–L56.

Nemiroff, R.J. (1989). On the probability of detection of a single gravitational lens. *Astrophysical Journal*, **341**, 579–587.

Nemiroff, R.J., Marani, G.F., Norris, J.P. and Bonnell, J.T. (2001). Limits on the cosmological abundance of supermassive compact objects from a millilensing search in gamma-ray burst data. *Physical Review Letters*, **86**, 580.

Newton, I. (1704). *Opticks, or a treatise of the reflections, refractions, inflections and colours of light*, 2nd edn, London.

Paczyński, B. (1986). Gravitational microlensing by the galactic halo. *Astrophysical Journal*, **304**, 1–5.

Paczyński, B. (1987). Giant luminous arcs discovered in two clusters of galaxies. *Nature*, **325**, 572–573.

Paczyński, B. (1996). Gravitational microlensing in the local group. *Annual Review of Astronomy and Astrophysics*, **34**, 419–460.

Perlmutter, S., Aldering, G., Goldhaber, G., Knop, R.A., Nugent, P., Castro, P.G., Deustua, S., Fabbro, S., Goobar, A., Groom, D.E., Hook, I.M., Kim, A.G., Kim, M.Y., Lee, J.C., Nunes, N.J., Pain, R., Pennypacker, C.R., Quimby, R., Lidman, C., Ellis, R. S., Irwin, M., McMahon, R.G., Ruiz-Lapuente, P., Walton, N., Schaefer, B., Boyle, B.J., Filippenko, A.V., Matheson, T., Fruchter, A.S., Panagia, N.,

Newberg, H.J.M. and Couch, W.J. (1999). Measurements of Omega and Lambda from 42 High-Redshift Supernovae. *Astrophysical Journal*, **517**, 565–586.

Peterson, B.M. (1997). *An Introduction to Active Galactic Nuclei*. Cambridge University Press.

Pospieszalska-Surdej, A., Surdej, J., Detal, A. and Jean C. (2000). The GL bibliography and an interactive database. In T.G. Brainerd and C.S. Kochanek (eds), *Gravitational Lensing: Recent Progress and Future Goals*, in the press.

Press, W.H. and Gunn, J.E. (1973). Method for detecting a cosmological density of condensed objects. *Astrophysical Journal*, **185**, 397–412.

Refsdal, S. (1964a). The gravitational lens effect. *Monthly Notices of the Royal Astronomical Society*, **128**, 295–306.

Refsdal, S. (1964b). On the possibility of determining Hubble's parameter and the masses of galaxies from the gravitational lens effect. *Monthly Notices of the Royal Astronomical Society*, **128**, 307–310.

Refsdal, S. (1965). Proc. Int. Conf. on Relativistic Theories of Gravitation, London.

Refsdal, S. (1966b). On the possibility of determining the distance and masses of stars from the gravitational lens effect. *Monthly Notices of the Royal Astronomical Society*, **134**, 315–319.

Refsdal, S. (1966a). On the possibility of testing cosmological theories from the gravitational lens effect. *Monthly Notices of the Royal Astronomical Society*, **132**, 101–111.

Refsdal, S. (1970). On the propagation of light in universes with inhomogeneous mass distribution. *Astrophysical Journal*, **159**, 357–375.

Refsdal, S. and Surdej, J. (1994). Gravitational lenses. *Reports on Progress in Physics*, **57**, 117–185.

Renn, J., Sauer, T. and Stachel, J. (1997). The origin of gravitational lensing: A postcript to Einstein's 1936 *Science* paper. *Science*, **275**, 184–186.

Riess, A.G., Filippenko, A.V., Challis, P., Clocchiatti, A., Diercks, A., Garnavich, P.M., Gilliland, R.L., Hogan, C.J., Jha, S., Kirshner, R.P., Leibundgut, B., Phillips, M.M., Reiss, D., Schmidt, B.P., Schommer, R.A., Smith, R.C., Spyromilio, J., Stubbs, C., Suntzeff, N.B. and Tonry, J. (1998). Observational evidence from supernovae for an accelerating universe and a cosmological constant. *Astronomical Journal*, **116**, 1009–1038.

Robertson, D.S., Carter, W.E., Dillinger, W.H. (1991). New measurement of solar gravitational deflection of radio signals using VLBI. *Nature*, **349**, 768–770.

Roukema, B.F. and Luminet, J-P. (1999). Constraining curvature parameters via topology. *Astronomy and Astrophysics*, **348**, 8–16.

Sackett, P.D. (2001). Microlensing and the physics of stellar atmospheres. In J.W. Menzies and P.D. Sackett (eds), *Microlensing 2000: A New Era of Microlensing Astrophysics*. ASP Conference Series, Astronomical Society of the Pacific, San Francisco (in press).

Sanitt, N. (1971). Quasi-stellar objects and gravitational lenses. *Nature*, **234**, 199–203.

Schmidt, M. (1963). 3C 273: A star-like object with large red-shift. *Nature*, **197**, 1040.

Schmidt, R. and Wambsganss, J. (1998). Limits on MACHOs from microlensing in the double quasar Q 0957 + 561. *Astronomy and Astrophysics*, **335**, 379–387.

Schneider, P. (1993). Upper bounds on the cosmological density of compact objects with sub-solar masses from the variability of QSOs. *Astronomy and Astrophysics*, **279**, 1–20.

Schneider, P., Ehlers, J. and Falco, E.E. (1992). *Gravitational Lenses*. Astronomy and Astrophysics Library, Springer-Verlag, Berlin.

Smail, I., Ivison, R.J. and Blain, A.W. (1997). A deep submillimeter survey of lensing clusters: A new window on galaxy formation and evolution. *Astrophysical Journal*, **490**, L5–L8.

Smette, A., Robertson, J.G., Shaver, P.A., Reimers, D., Wisotzki, L. and Köhler, Th. (1995). The gravitational lens candidate HE 1104-1805 and the size of absorption systems. *Astronomy and Astrophysics*, Suppl., **113**, 199–236.

Smette, A., Surdej, J., Shaver, P.A., Foltz, C.B., Chaffee, F.H., Weymann, R.J., Williams, R.E. and Magain, P. (1992). A spectroscopic study of UM 673 A and B: On the size of Lyman-α clouds. *Astrophysical Journal*, **389**, 39–62.

Soldner, J. (1804). Über die Ablenkung eines Lichtstrahls von seiner geradlinigen Bewegung durch die Attraktion eines Weltkörpers, an welchem er nahe vorbeigeht. *Berliner Astronomisches Jahrbuch*, 161–172.

Soucail, G., Fort, B., Mellier, Y. and Picat, J-P. (1987). A blue ring-like structure in the center of the A 370 cluster of galaxies. *Astronomy and Astrophysics*, **172**, L14–L16.

Soucail, G., Mellier, Y., Fort, B., Mathez, G. and Cailloux, M. (1988). The giant arc in A 370: Spectroscopic evidence for gravitational lensing from a source at $z = 0.724$. *Astronomy and Astrophysics*, **191**, L19–L21.

Surdej, J., Claeskens, J-F. (1997). Gravitational lens studies with a LMT. In M. Ferrari (ed.), Proceedings of international workshop on 'Science with Liquid Mirror Telescopes', Marseille Observatory, 14–15 April 1997. see the url: http://wood.phy.ulaval.ca/Workshop/Wproceed.html#Surdej

Surdej, J., Claeskens, J-F., Crampton, D., Filippenko, A.V., Hutsemékers, D., Magain, P., Pirenne, B., Vanderriest, C. and Yee, H.K.C. (1993). Gravitational lensing statistics based on a large sample of highly luminous quasars. *Astronomical Journal*, **105**, 2064–2078.

Surdej, J., Claeskens, J-F., Remy, M., Refsdal, S., Pirenne, B., Prieto, A., Vanderriest, Ch. (1997). HST confirmation of the lensed quasar J03.13. *Astronomy and Astrophysics*, **327**, L1–L4.

Surdej, J., Magain, P., Swings, J-P., Remy, M., Borgeest, U., Kayser, R., Refsdal, S., Kühr, H. (1988). Preliminary results from a search for gravitational lensing within a sample of highly luminous quasars. In C. Balkowski and S. Gordon (eds), *Large Scale Structures: Observations and Instruments*, Proceedings of the 1st DAEC [Département d'Astrophysique Extragalactique et de Cosmologie] Workshop, Paris, pp. 97–107.

Treuhaft, R.N. and Lowe, S.T. (1991). A measurement of planetary relativistic deflection. *Astronomical Journal*, **102**, 1879–1888.

Turner, E.L. (1980). The effect of undetected gravitational lenses on statistical measures of quasar evolution. *Astrophysical Journal*, **242**, L135–L139.

Turner, E.L. (1990). Gravitational lensing limits on the cosmological constant in a flat universe. *Astrophysical Journal*, **365**, L43–L46.

Turner, E.L., Ostriker, J.P. and Gott, J.R. III (1984). The statistics of gravitational lenses: The distributions of image angular separations and lens redshifts. *Astrophysical Journal*, **284**, 1–22.

Tyson, J.A. (1988). Deep CCD survey – Galaxy luminosity and color evolution. *Astronomical Journal*, **96**, 1–23.

Tyson, J.A., Wenk, R.A. and Valdes, F. (1990). Detection of systematic gravitational lens galaxy image alignments: Mapping dark matter in galaxy clusters. *Astrophysical Journal*, **349**, L1–L4.

Vanderriest, C., Schneider, J., Herpe, G., Chèvreton, M., Moles, M. and Wlérick, G. (1989). The value of the time delay $\Delta T$ (A, B) for the 'double' quasar 0957 + 561 from optical photometric monitoring. *Astronomy and Astrophysics*, **215**, 1–13.

Van Waerbeke, L., Mellier, Y., Erben, T., Cuillandre, J.C., Bernardeau, F., Maoli, R., Bertin, E., McCracken, H.J., Le Fèvre, O., Fort, B., Dantel-Fort, M., Jain, B. and Schneider, P. (2000). Detection of correlated galaxy ellipticities on CFHT data: first evidence for gravitational lensing by large-scale structures. *Astronomy and Astrophysics*, **358**, 30–44.

Wallington, S., Kochanek, C.S. and Narayan, R. (1996). LensMEM: A gravitational lens inversion algorithm using the maximum entropy method. *Astrophysical Journal*, **465**, 64–72.

Wallington, S. and Narayan, R. (1993). The influence of core radius on gravitational lensing by elliptical lenses. *Astrophysical Journal*, **403**, 517–529.

Walsh, D., Carswell, R.F. and Weymann, R.J. (1979). 0957 + 561 A, B: twin quasi-stellar objects or gravitational lens? *Nature*, **279**, 381–384.

Wambsganss, J. (1998). Gravitational lensing in astronomy. *Living Reviews in Relativity*, **1**, No. 1998-12. [This is an electronic journal; the url is http://www.livingreviews.org]

Wilkinson, P.N., Henstock, D.R., Browne, I.W.A., Polatidis, A.G., Augusto, P., Readhead, A.C.S., Pearson, T.J., Xu, W., Taylor, G.B. and Vermeulen, R.C. (2001). Limits on the cosmological abundance of supermassive compact objects from a search for multiple imaging in compact radio sources. *Physical Review Letters*, **86**, 584–587.

Wittman, D.M., Tyson, J.A., Kirkman, D., Dell'Antonio, I. and Bernstein, G. (2000). Detection of large-scale cosmic dark matter structure via gravitational lens distortion. *Nature*, **405**, 143–148.

Wolfe, A.M. (1988). Damped Ly-alpha absorption systems. In: *QSO Absorption Lines: Probing the Universe*; Proceedings of the QSO Absorption Line Meeting, Baltimore, MD, 19–21 May 1987, Cambridge University Press, pp. 297–306.

Young, P., Gunn, J.E., Oke, J.B., Westphal, J.A. and Kristian, J. (1981). Q0957 + 561: detailed models of the gravitational lens effect. *Astrophysical Journal*, **244**, 736–755.

Zwicky, F. (1937a). Nebulae as gravitational lenses. *Physical Review*, **51**, 290.

Zwicky, F. (1937b). On the probability of detecting nebulae which act as gravitational lenses. *Physical Review*, **51**, 679.

Zwicky, F. (1957). *Morphological Astronomy*, Springer, Berlin.